DEPARTMENT OF CHEMISTRY, UNIVERSITY OF JYVÄSKYLÄ

RESEARCH REPORT No. 66

DEVELOPMENT OF A METHOD BASED ON LASER-INDUCED PLASMA SPECTROMETRY FOR RAPID SPATIAL ANALYSIS OF MATERIAL DISTRIBUTIONS IN PAPER COATINGS

BY
HEIKKI HÄKKÄNEN

Academic Dissertation
for the Degree of
Doctor of Philosophy

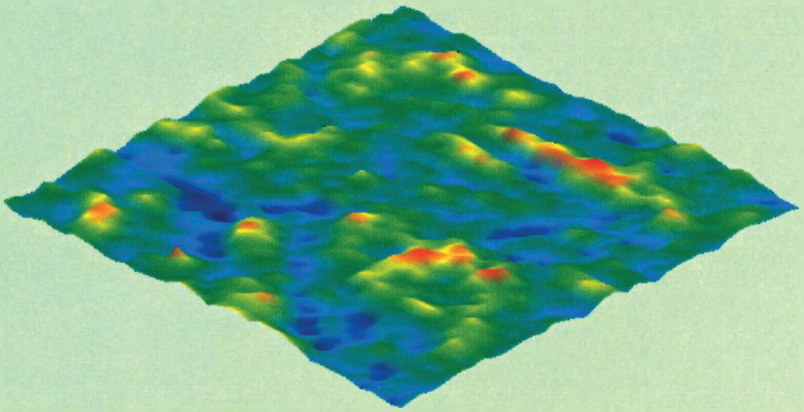

Jyväskylä, Finland 1998
ISBN 951-39-0280-3
ISSN 357-346X

DEPARTMENT OF CHEMISTRY, UNIVERSITY OF JYVÄSKYLÄ

RESEARCH REPORT No. 66

DEVELOPMENT OF A METHOD BASED ON LASER-INDUCED PLASMA SPECTROMETRY FOR RAPID SPATIAL ANALYSIS OF MATERIAL DISTRIBUTIONS IN PAPER COATINGS

BY

HEIKKI HÄKKÄNEN

Academic Dissertation
for the Degree of
Doctor of Philosophy

To be presented by the permission of the Faculty of Mathematics and Natural Sciences of the University of Jyväskylä, for public examination in auditorium KEM 4 on 1.7.1998, at12 o´clock noon.

Copyright ©,1998
University of Jyväskylä
Jyväskylä, Finland
ISBN 951-39-0280-3
ISSN 0357-346X

URN:ISBN:978-951-39-9927-8
ISBN 978-951-39-9927-8 (PDF)
ISSN 0357-346X

University of Jyväskylä, 2024

Dedicated

to my sons

KALLE and JUSSI.

PREFACE

The present studies were carried out in the department of Chemistry, University of Jyväskylä during the years 1990-1998 under supervision of Prof. Jouko Korppi-Tommola whom I owe my gratitude for his support, guidance and encouragement throughout these years.

I would like to thank the students who have participated to this work for their help and innovative discussions: Timo Peltola, Jukka Lavikainen, Juha Houni, and Janne Ihalainen. I am grateful to Erkki Järvinen and Tapani Sorsa for their technical assistance in building the experimental set-up. Thanks to the colleges for the refreshing moments spent in the coffee room. Thanks also to numerous people in the paper industry for showing interest on my research, which have given me courage to go on. Special thanks goes to Vesa Helenius for criticisms, discussions and for his valuable help both in the work and free time. I would like to thank Noël Smith Roger for proof reading the theses. The studies have been support by Technology Development Center (TEKES), Ministry of Education, Jyväskylä Science Park Ltd, which are acknowledged.

My deepest gratitude goes to my wife Riitta for her patience and understanding for all my absence and excuses; Thank You.

Jyväskylä, June 1998

Heikki Häkkänen

ABSTRACT

A rapid and low-cost analytical method for studying the material distributions of paper coatings has been developed. The method operates in the dimensional scale of a raster point in printing (≈0.1 mm) and on the other hand it is capable of mapping areas the size of several square centimeters. The results have been used to explain functional properties of paper, especially visual appearance and printability.

An instrument based on laser-induced plasma spectroscopy (LIPS) has been constructed. In this method a pulsed laser beam is focused onto the paper surface at irradiance greater than 0.1 GW/cm^2. A small amount of material (10-100 ng), depending on energy of laser pulse and material, is ablated and excited by a single laser pulse to produce a plasma. The plasma emits an atomic emission spectrum which represents the elemental composition of the sample. Typically an area of 0.1 mm in diameter and 2 μm in depth is ablated by a single laser pulse from the paper surface. The depth profile of elemental compositions is obtained by consecutive measurements in the same XY-location. Larger areas have been analyzed by translating the sample with respect to the laser focus. In this way three dimensional elemental distribution maps have been constructed.

In this study the LIPS-method has been utilized in the analysis of the properties characteristic of papers: coat weight, coating coverage, pigment compositions, binder/pigment-ratio, and the relative distribution of coatings in multilayer coatings. The filler distributions of uncoated papers have also been studied.

CONTENTS

ABBREVIATIONS

AES	Atomic emission spectrometry
ATR	Attenuated total reflectance
CCD	Charge coupled device
DCC	Degree of coating coverage
EDXA	Energy dispersive X-ray analysis
ESCA	Electron spectroscopy for chemical analysis
IR	Infrared
LA	Laser ablation
LIBS	Laser-induced breakdown spectroscopy
LIF	Laser-induced fluorescence
LIPS	Laser-induced plasma spectroscopy
LWC	Light weight coated
MWC	Medium weight coated
PCC	Precipitated calcium carbonate
PMT	Photo multiply tube
pph	Parts per hundred
RSD	Relative standard deviation
SB	Styrene-butadiene
SEM	Scanning electron microscope
SC	Supercalendered
TRE-LIBS	Time resolved laser-induced breakdown spectroscopy

1 INTRODUCTION

There has been a demand for a rapid, low-cost method for analysing material distribution in paper coatings. The method needs to operate on a sufficiently small scale (the raster point in printing is <0.1 mm) but on the other hand it should be capable of mapping areas of several square centimeters. The results should correlate with the functional properties of paper, especially with visual appearance and imprint.

The aim of the present thesis was to study paper properties by using a XeCl-excimer laser. The intense, pulsed laser beam at a wavelength of 308 nm can be used in different ways and diverse information can be obtained from the paper surface. The study of material distributions began by using the laser-induced fluorescence (LIF) technique. The intensity of the fluorescence signal is dependent on the concentration of fluorescent molecules (mainly optical brighteners) in the coating or on the amount of coating masking the fluorescence from optical brighteners in the base paper. The main result was that the LIF-method is feasible as an on-line method for studying coat weight distributions of certain paper grades.

The paper coating can be ablated to form plasma by using an intense laser pulse. The elemental content of the sample can be evaluated by laser-induced plasma spectrometry (LIPS). Early stages of this work using LIPS was only meant to confirm results obtained by LIF, but the method turned out to be superior since it offered an opportunity for 3-dimensional mapping of elemental compositions in paper coatings. Also the distribution of fillers in paper were analyzed.

The work may be divided in two parts. In the first place there was the development of an automated analysis instrument. The other part of the work was a study of the physics lying behind the measurements and the realization of the opportunities and restrictions of the methods in the analysis of paper.

2 MATERIAL DISTRIBUTIONS IN PAPER

Paper

Paper consists of small cellulose fibers which are bound together by hydrogen bonds. In some grades inorganic pigments (fillers) are added in order to improve the opacity and surface properties of paper. Paper may be coated by a porous layer of pigments and adhesives to further improve its surface properties. The purpose of coating is to fill voids of the base paper and give a smooth surface. Pigment coatings are normally applied to the base paper in the form of water suspensions. The total solids content of the suspension, i.e. pigment plus adhesive, may be 35-70% by weight. After application, the coating is dried by the removal of water from the film. In some cases the paper is calendered to further smoothen the surface and develop a glossy finish.

There are two main properties that characterize the quality of paper surface. The first is topography, i.e. how smooth the surface is, and the second is distribution of materials in the paper surface. An uneven distribution of materials, e.g. migration of binder, may cause mottling which can been seen in a paper as an uneven imprint or gloss. A microscope image of a stained cross section of multilayer coated paper is shown in Fig 2.1.

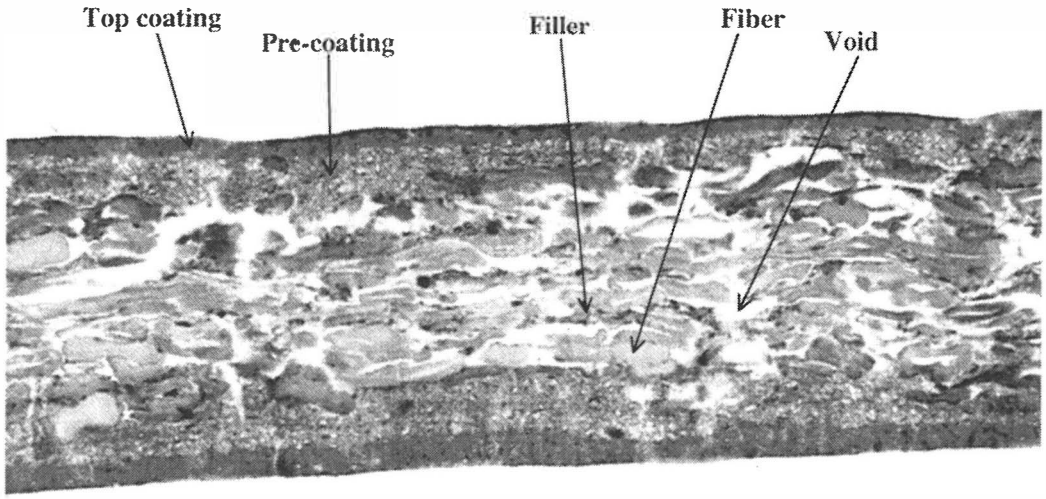

Figure 2.1. A cross section of multilayer coated paper.

Pigment

In papermaking the pigments primarily used are kaolin, calcium carbonate and to a minor extent talc and titanium dioxide. Pigments comprise 75-90% of the dry solids in paper coatings. The particle sizes of coating pigments vary from 50 μm to 0.1 μm. Particle size distribution depends on where it is used, for a top coating finer pigment are used than for a pre-coating. Pigment particles fill the spaces between fibers on the sheet surface and form a nearly uniform surface mat. Pigments also control opacity, gloss, and the color of the raw stock. Refractive index, particle size, crystal structure, light scattering and absorption, and adhesive demand are important characteristics of pigments. Minor amounts of impurity minerals can adversely affect pigment properties.

Kaolins are hydrated alumino silicates having the generalized formula ($Al_2O_3 \cdot 2SiO_2 \cdot 2H_2O$). Kaolin particles occur as natural hexagonal plates with a aspect ratio of *ca* 10. Calcium carbonate is available from natural sources (GCC), but also precipitated forms (PCC) are used. Calcium carbonate is often used with kaolin to produce improved brightness and to increase printability and ink receptivity it has also better runnability at higher solid contents compared to kaolin. The calcium carbonate pigment is not plate-shaped and it disrupts the orientation of the kaolin plates, reduces the surface gloss and maintains the porosity of the coating. It is a common component of matte-finish coatings.

Talc is also a silicate mineral having the formula ($3MgO \cdot 4SiO_2 \cdot H_2O$). It has a large average particle size with particle diameter-to-thickness ratio of *ca* 30-40:1. It is mainly used in rotogravure grades. Titanium dioxide is used in coatings because of its high refractive index to improve opacity and brightness. Pigments used as fillers of paper are similar to the pigments used in paper coatings. The particle size is larger though in fillers.

Binder

The primary function of adhesives in the pigment coating is to bind the pigment particles together and to the base paper. The type and proportion of the binder controls many of the characteristics of the finished paper, e.g., surface strength, gloss, brightness, opacity, smoothness, ink receptivity, and firmness of surface. The amount of adhesives in a coating

formulation varies from about 5 to 25%, depending on the pigment. Commonly used binders are starch, styrene-butadiene, acrylates and polyvinyl acetate.

Analysis of material distributions in coated paper

Commonly measured material distributions of paper are mass distribution, filler distribution, coatweight distribution, binder distribution[1], and distribution of pigments.[2]

Mass distribution of paper is most commonly analyzed by absorption of β-radition. Another technique reported is light transmission coupled with computer based image analysis.[3] Distribution of pigments is measured by x-ray absorption (ash). All these methods use transmission of radiation through the paper and give a picture of material distributions in xy-direction through the paper. Coat weight variations have also been analysed using image analysis of burn-out samples.[4] The coating may be removed in thin layers by abrasion or grinding and the material distributions (binder / pigment ratio) can be measured by surface analysis methods like multiple internal reflectance (MIR) infrared spectroscopy, attenuated total reflectance (ATR- IR), and electron spectroscopy for chemical analysis (ESCA)[5]. UV-absorption has been used to measure distribution of SB-latex in coatings.[6]

Cross sectioning of paper allows the material distribution in the z-direction to be determined. Methods like scanning electron microscopy (SEM) combined with energy dispersive X-ray analysis (EDXA)[7,8], Raman spectroscopy[9] and optical microscopy combined with image analysis have been used for analysis of material distributions in cross sections. SEM combined with backscattering electron imaging is used to evaluate coating coverage.[10]

The LIPS-method presented in this work is a new and promising method for the analysis of material distributions in paper and paper coatings.

3 LASER-INDUCED PLASMA SPECTROMETRY

Laser-induced plasma spectrometry (LIPS) is an elemental analysis method based on the atomic emission of laser-produced plasma. It is also known as *laser-induced breakdown spectrometry* (LIBS) or *Laser ablation atomic emission spectrometry* (LA-AES). Two years after the invention of the laser it was proposed by Brech and Cross (1962)[11] that a laser pulse focused to a sufficiently high irradiance can generate a plasma useful for spectrochemical analysis. Quite a lot of work was done from the sixties to the eighties in applying the method in the study of several materials: metals, molten metals, minerals, ores, art work, paints, environmental samples etc. These studies and the characteristics of the method are discussed in several reviews.[12-17] Lasers and detection systems have developed during the last decade and the cost of the equipment is now at a more reasonable level. In the nineties mainly Nd:YAG and excimer lasers have been used in applications of LIPS and light emission has been detected by photomultiplier tubes, photodiode arrays, and CCDs. With the latter two detectors, image intensifiers are often used to allow time resolved measurements.

LIPS can be used to analyze samples in all phases: solid, liquid, and gas. Main advantages of using LIPS are the minimal sample preparation, rapid simultaneous analysis of elements, the possibility of mapping local concentrations in inhomogenous materials like minerals and thin films, and the relatively low cost of investigation. The feasibility of the use of a portable instrument has also been demonstrated.[18]

The fields where the method may be profitably used are spatial analysis and analysis in hostile environments e.g. at nuclear power stations, because only optical access to the target is needed. The LIPS system has been used for monitoring and screening in environmental science, industrial hygiene and various production processes.[19-20]

Interaction of laser with material

When a high irradiance (>0.1 GW/cm^2) laser pulse interacts with a sample a short-lived plasma is produced. There are two main mechanisms for the plasma formation. The first one is inverse *Bremsstrahlung,* i.e. the electrons absorb laser radiation simultaneously as they collide with neutral atoms and photon energy is converted into the kinetic energy of the electron. The reaction is as follows

$$M + e + h\nu \rightarrow M + e \qquad 3.1$$

where M is atom, e is electron, and hν denotes photon energy where h is Planck´s constant and ν is frequency. If the electrons gain sufficient kinetic energy, they can impact to ionize an atom through the reaction with an atom

$$e + M \rightarrow 2e + M^{+} \qquad 3.2$$

The second mechanism is multiphoton ionization i.e. an atom or molecule absorbs simultaneously a sufficient number of photons to result in ionization.

$$M + mh\nu \rightarrow M^{+} + e \qquad 3.3$$

m is number of photons. Both mechanisms are involved in the laser ablation process. The mechanism is dependent on the wavelength of the laser, target material, thr surrounding gas and its pressure.

The excitation of atoms occurs by absorption of laser light

$$M + h\nu \rightarrow M^{*} \qquad 3.4$$

or by collisions of electrons with neutrals

$$M + e \rightarrow M^{*} + e \qquad 3.5$$

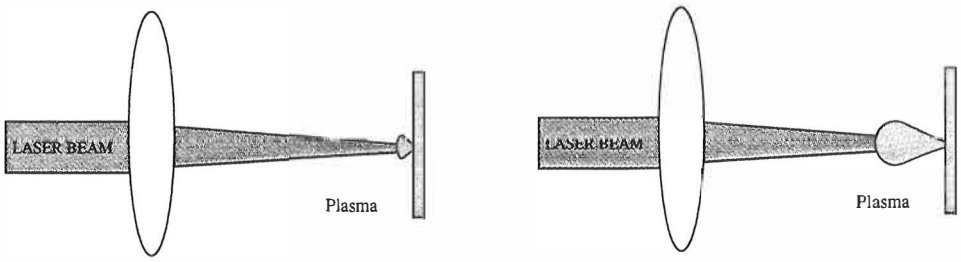

Figure 3.1. Generation of plasma by focusing a laser beam onto the sample surface at the early stages of excitation (A) and at the end of the excitation when plasma is heated mainly by inverse bremsstrahlung (B).

Wavelengths from 1064 nm (fundamental of Nd:YAG laser) to 193 nm of ArF excimer laser have commonly been used to produce plasma in LIPS-experiments. The mechanism of plasma formation is dependent on wavelength. In the near infrared region (NIR) the main mechanism of plasma formation is inverse *Bremsstrahlung*. In the UV multiphoton ionization dominates. The number of photons required for ionization depends on the ionization potential of the material. Organic molecules are often ionized by a single UV-photon and inorganics require a couple of photons. It has also been observed by using NIR-radiation that the ablated mass is independent of pulse energy under certain conditions, but in the UV the ablated mass is correlated to pulse energy.[21] NIR-behaviour is due to the interaction of laser with plasma. When the electron density (n_e) is high enough the plasma turns out to be opaque and no laser radiation reaches the target. The light is reflected from plasma if its wavelength is greater than the wavelength of plasma (λ_p).[14,22]

$$\lambda_p \cong 10^{-15}(n_e)^{1/2} \qquad 3.6$$

Light emitted by plasma

During the impact of laser pulse the plasma temperature rises above 10 000 K. At the early stages of excitation, a featureless continuum, owing to the *Bremsstrahlung* and recombination reactions, is observed. With time, the intensity of the continuum decreases and the emission lines of the ions become visible. At later times lines from neutral atoms start to dominate the spectrum. In the LIPS analysis the neutral atom lines are monitored to give the elemental constituents of the target sample.

The time evolution of the LIPS-spectrum of an aluminum sample is shown in figure 3.2. The emission decays fast owing to the low energy used for excitation. By using more energetic excitation,0 emission may last tens of microseconds.

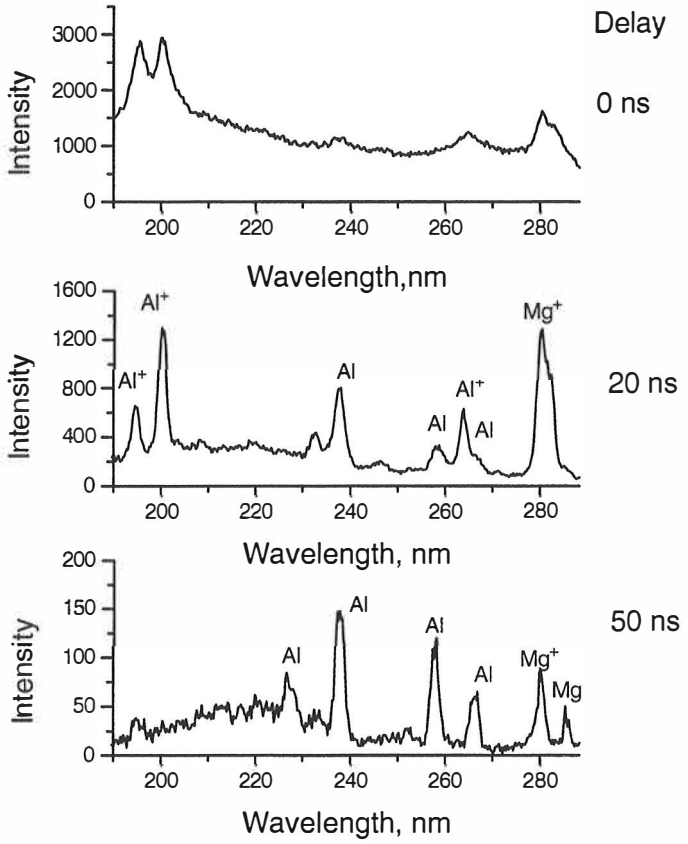

Figure 3.2. Effect of time delay on LIPS-spectra of aluminum. (Note the different intensity scales)

The continuum of the LIPS spectrum is due to *Bremsstrahlung* and recombination of electrons and ions

$$M + e \rightarrow M + e + h\nu \qquad 3.7$$

$$M^+ + e \rightarrow M + h\nu \qquad 3.8$$

The emission lines of the spectrum originate from transitions between electronic levels of atoms or ions in the plasma.

$$M^* \rightarrow M + h\nu \qquad 3.9$$

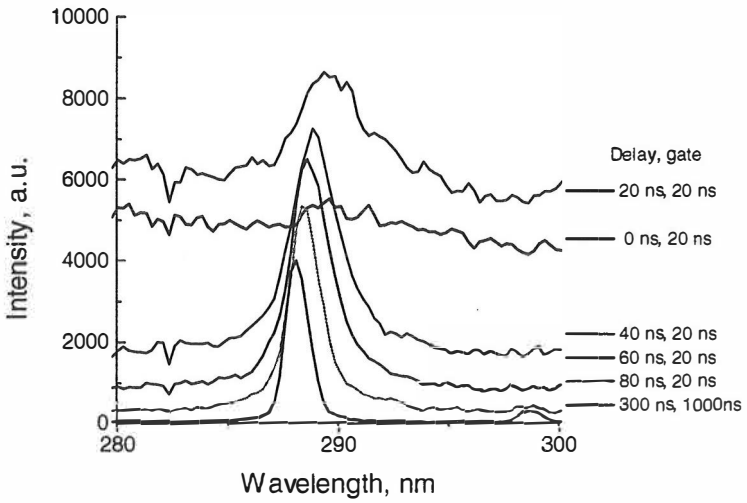

Figure 3.3. Time evolution of the line width and shift of the Si(I) line at 288.1 nm.

Emission lines are broadened in a hot plasma. This is mainly due to collisions, Doppler and Stark effects. The Stark effect also gives rise to a red shift of the spectral line.[23] The spectral broadening and shift of Si transition $3s^2 3p4s \rightarrow 3s^2 3p^2$ at 288 nm is shown in Fig. 3.3. Lines become narrower with time as the plasma cools. The shift of emission lines may lead to incorrect results if too narrow a spectral window is used in the temporal analysis.

Resonance lines, i.e. transitions between the excited state and the ground state, may suffer from absorption of the ground state atoms in the plasma. That process is known as self-absorption. An example of this is shown in Section 5.1 Fig 5.3.

Asymmetrical self-absorption can be explained in terms of Doppler effect. The absorbing atoms form part of the radially expanding outer zone of the plasma and the emission originating from atoms between the center of hot plasma and the detector may be absorbed. The emission of atoms drawing away from the detector is seen in the spectrum on the red side of the broadened line in Fig. 3.4 at a delay of 40 ns. Self-reversal of Cu doublet transition $3d^{10}4p^1 - 3d^{10}4s^1$ is seen at delay of 20 ns as a dip in the continuum spectrum. Such an effect is due the absorption of continuum emission by ground state atoms.

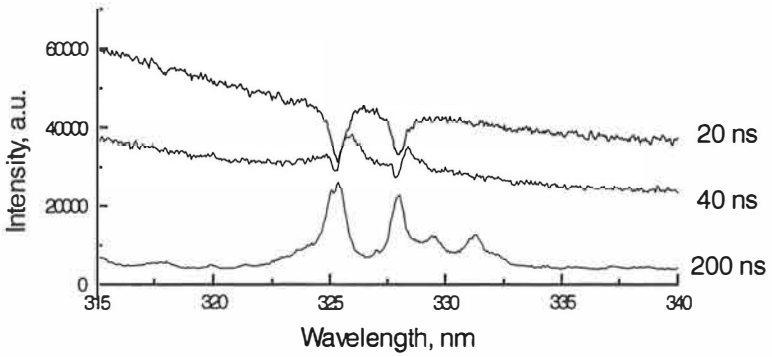

Figure 3.4. Self-reversal of Cu doublet transition $3d^{10}4p^1$ - $3d^{10}4s^1$.

Because of self-absorption, it is not recommended to use resonance lines in quantitative analysis, but for trace elements they are the only lines that can be seen. In this case the concentration of atoms is so low that no self-absorption will occur.

Electron temperature of the plasma

The electron temperature T_e of the plasma can be estimated by using the Bolzmann distribution law

$$\ln(I\lambda/Ag) = -E/kT_e \qquad 3.10$$

where I is intensity, λ is wavelength, A is transition probability, g and E are the statistical weight and the energy of the upper state, respectively, and k is Bolzmann's constant. To obtain T_e ln ($I\lambda$ /gA) is plotted as a function of energies of the upper states of transitions for a number of spectral emission lines. The plot will give a straight line of slope ($-1/kT_e$) from which the electron temperature can be calculated. Typically the value of T_e is >10 000 K in the early stages of plasma formation. The equation is valid only if the local thermodynamical equilibrium (LTE) exists, i.e. the collisions dominate in the energy transfer reactions establishing a Bolzmann distribution.[24]

4 EXPERIMENTAL

The experimental set-up developed in this work is shown in Fig 4.1. The laser-induced plasma spectrometer consists of three main components: (i) a light source and a system to monitor and control laser pulse energy (ii) a sample translation stage, and (iii) a spectrometer with time resolved multichannel detection system. The latest version of the set-up is described in detail and the development of the measuring system during various stages of the work is briefly explained. The earlier versions of the system are presented in previous articles in more detail.[25-27]

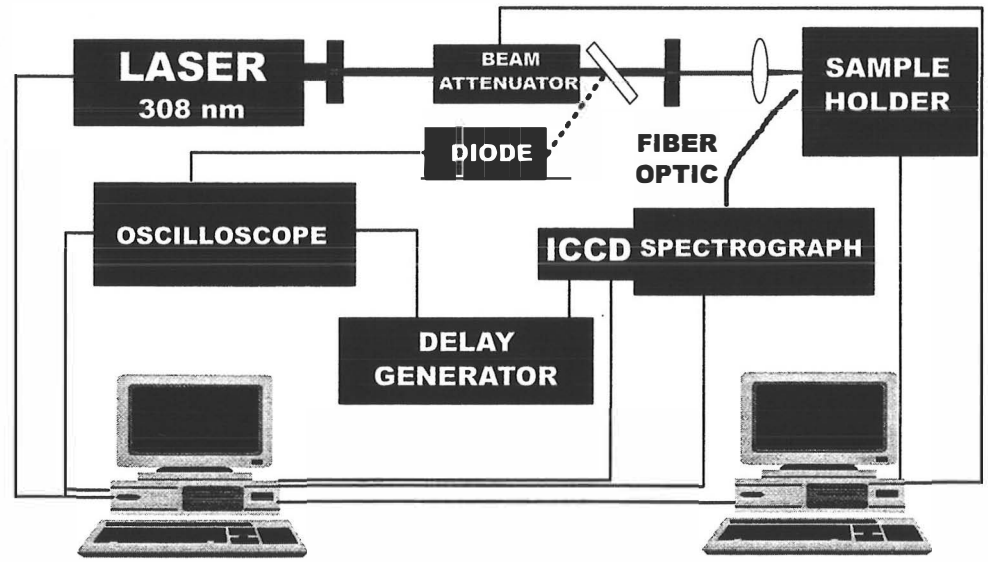

Figure 4.1. Schematic presentation of the experimental set-up

Light source

XeCl-excimer lasers (ELI-5M, Estonian Academy of Sciences and EXC-150/25 Estla Ltd) emitting 60 mJ pulses at the wavelength of 308 nm with 15 ns pulse duration were used as light sources. The laser energy was adjusted by a computer controlled beam attenuator, which consisted of a stepper motor and two filters (wg 280, Schott), which may be tilted with

respect to the laser beam in order to attenuate the energy. The filters were turned simultaneously in opposite directions. The design preserves the laser beam path while attenuating the intensity. Schematic presentation of the beam attenuator is shown in figure 4.2.

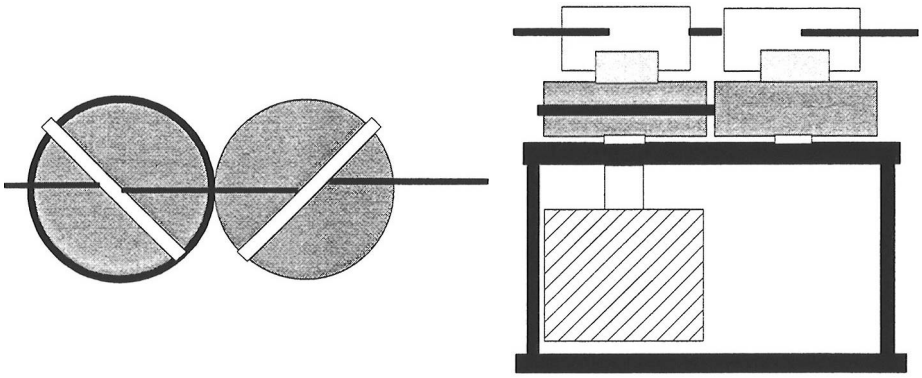

Figure 4.2. The beam attenuator.

Coarse adjustment of the laser energy was done by using apertures of 2-5 mm in diameter. The laser pulse energy was frequently measured with a power meter (Gentec Inc., ED 104) and continuously monitored by a photodiode (DET 200, Thorlabs Inc.) and a digital oscilloscope (Tektronix TDS 520 C). In this way long term drift of the laser and shot-to-shot intensity fluctuations could be accounted for. The laser beam was focused onto the surface of the paper sample at normal incidence by a 50-mm-focal-length quartz lens. The spot size on the paper surface was varied between 30-250 μm in diameter by altering the distance between the focusing lens and the sample surface. The focal point was offset towards the inside of the sample to avoid thermal lensing and light scattering from air at the focal area.

The power density on the sample was typically set to 0.3 GW/cm^2 and used in each experiment by varying pulse energies from 0.2 mJ to 9 mJ depending on the spot diameter. Measurements were carried out in atmospheric pressure by blowing buffer gases like N_2 or Ar onto the focal area.

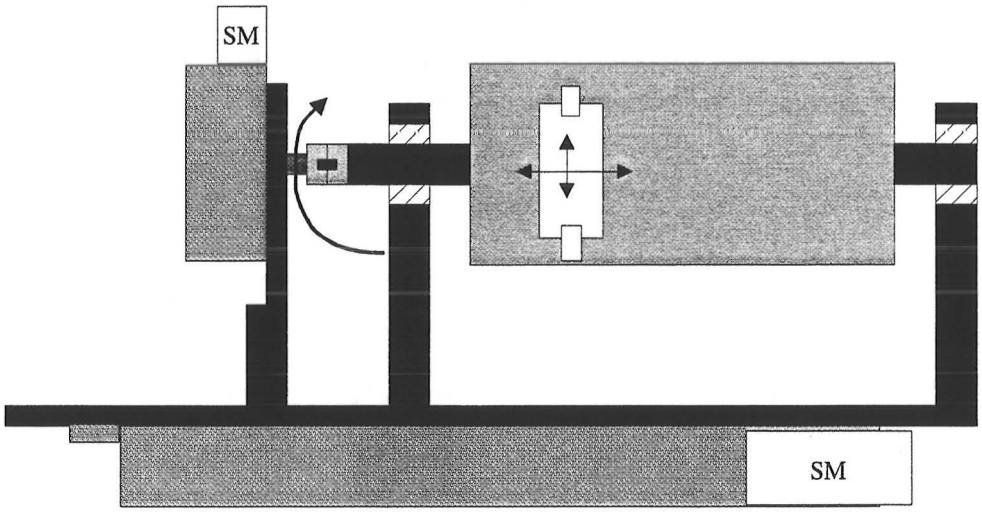

Figure 4.3. Sample holder(SM = stepper motor).

Sample holder

The sample holder is an aluminum cylinder 220 mm in length and 100 mm in diameter. An A4 paper sheet can be conveniently attached on the outside surface of the cylinder. It was designed to fit an A4 paper sheet as the largest sample. Alternatively, several paper stripes may be attached to the cylinder by using adhesive tape. The position of the laser focus on the sample was controlled by rotating and translating the cylinder with stepper motors. Minimum translation step size is 10 μm. Stepping of the motors was controlled by a computer. The sample holder is illustrated in figure 4.3.

Spectrometer with gated multichannel detection

The light from the plasma plume was collected and transmitted to the spectrograph via a fiber optic bundle (Oplatek Oy). The bundle is 1 m long and 1 mm in diameter. The circular end of the bundle was placed 10 mm away from the plasma and the rectangular end (dimensions 7 x 0.15 mm) was placed in front of the spectrograph entrance slit. The light was collected at 45 degree angle with respect to the sample surface. Light emitted by plasma was dispersed in a 150 mm focal length imaging Czerny-Turner spectrograph (Acton Research Corporation, SP-150). Two gratings of 2400 and 600 lines/mm (blazed at 200 nm) provided the resolutions

and spectral coverages of about 0.2 nm and 30 nm or 0.8 nm and 120 nm. The spectrograph could be fully controlled by a computer program provided by the manufacturer.

The spectrally resolved light was detected by a gated intensified CCD detector (Oriel, InstaSpec V). It has a 1024×256 pixel CCD-chip and 18 mm image intensifier (illuminated area being 690×256 pixels). The spectral range of the ICCD is 180-850 nm. In the present studies mainly two spectral ranges 185-220 nm, and 275-302 nm were used.

The time delay and detection window of the measurement were adjusted by a digital delay/ pulse generator (Stanford Research Systems, DG 535). The delay generator was triggered from the output of a photo diode monitoring the laser pulse energy. Typical gate and delay times were 50 ns and 100 ns, respectively.

In fluorescence measurements the laser was fired by the delay generator and the fluorescent light was detected with in a 50 ns time window at the time of excitation.

Description of the software

The measurements were carried out using a computer program written by the author in C++ under DOS operating system. The input parameters of the program include total number positions to be sampled on the surface, distances between positions in x- and y-directions, respectively, and the number of pulses at each position. It is possible to automatically study several samples, one after another, by using a program "MULTI". For this program additional input parameters, i.e. the number of samples and the distance between the samples, have to be given. The program for data acquisition, initial data handling and the storing of the spectral data were written with the software provided by the manufacturer of the detector. The average energy of the laser pulse was kept constant during the measurement of a single sample series. The mean energy of 32 pulses was continually calculated and used as a measure of stability of the laser. When a deviation from the fixed value was more than 2 % an adjustment of the laser pulse intensity was carried out by using the computer controlled attenuator. Using a digital oscilloscope pulse-to-pulse intensity variation can now be recorded and intensity correction can be made at a later time.

Evolution of the measuring system

In the earlier versions of the LIPS-spectrometer, photomultiplier tubes (PMT) and a digital boxcar integrator (Model BX-531, NF Electronic Instruments) were used to detect plasma emission. During the earliest experiments only one monochromator was used. Later on a second monochromator was added to the system, which then allowed simultaneous monitoring of two elements. The disadvantage of using the boxcar integrator was that a minimum of 8 pulses was required for each data point to be stored in the memory. This put restrictions on the accuracy obtainable in the resolution of the surface analysis. The spatial resolution was restricted to eight times the diameter of the crater created by the laser pulse. In the present ICCD system the XY-resolution is limited by a single crater diameter. It also allows multilayer studies to be carried out more conveniently.

The other disadvantage in using PMT was the saturation of the PMTs near the laser line or in the regions with intensive fluorescence. Using the CCD a spectrum from each laser pulse is obtained, and the image intensifier allows the illumination of the detector only during a predefined moment (gate and delay times). It is then possible to get rid of the plasma continuum and fluorescence light, which overlap the atomic emission lines, especially at early times of detection.

Data handling and visualization

Spectral data were stored as background corrected integrated intensities of the emission lines of interest. The intensities were saved in a matrix format each element in its own file. In data handling commercial programs like Microcalc Origin, and Matlab have been used. In early stages of the work programs for visualization of the results were written using C programming language in PC and in Silicon Graphics environments.

5 RESULTS AND DISCUSSION

5.1 GENERAL CONSIDERATIONS OF LIPS-ANALYSIS

In order to optimize the LIPS method for the analysis of inhomogenous samples such as paper, many different factors had to be considered. Some parameters affecting the intensity of spectral lines and the amount of mass ablated by laser pulse are shown in Fig. 5.1. These factors can be divided in to three categories: excitation, environment and target properties. In this chapter each of these is discussed in detail.

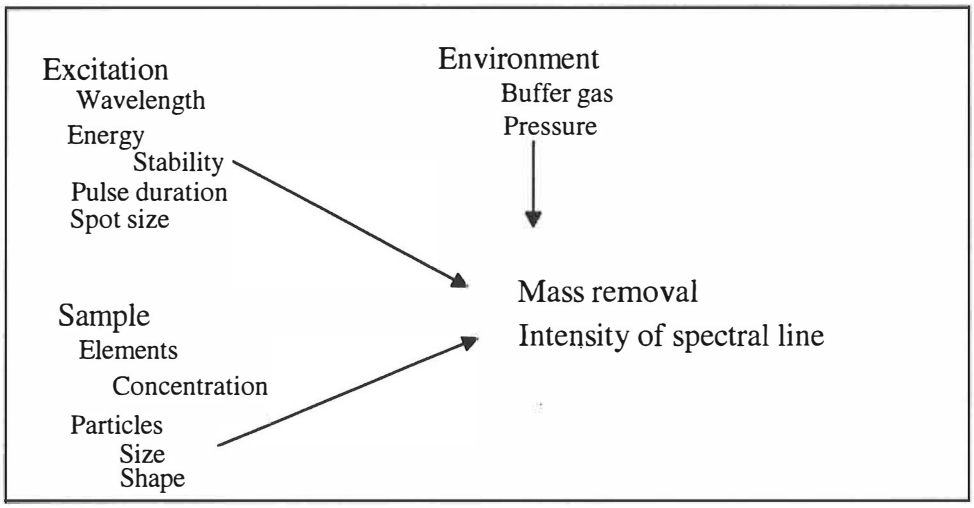

Figure 5.1. Parameters affecting mass removal and intensity of spectral lines in LIPS analysis of solid inhomogenous materials.

Optimizing excitation parameters

The excitation parameters like wavelength and pulse duration are restricted by the kind of laser that is available. For the present work we have used a XeCl-excimer laser operating at 308 nm giving 15 ns pulses with maximum pulse energy of 60 mJ. The laser ablation process requires sufficient irradiance at the sample surface. The threshold irradiance of ablation is dependent on material, and typically it is around 10^8 W/m^2. Laser pulses of short duration with the same irradiance ablate less material than longer pulses, i.e. the duration of laser pulse determines the minimum depth of the crater created (resolution in z-direction). The amount of ablated material is dependent on pulse energy. The intensities of atomic emission lines

depend on the amount of material in the plasma. The sensitivity of the detection system determines the minimum amount of material that can be ablated from the surface. If low pulse energy is used to create the plasma the decay time of emission is short, because the plasma cools faster than when high pulse energy is used.

The wavelength of the laser affects the characteristics of plasma. UV-ablation produces relatively cold plasma i.e., plasma consist mostly of neutral atoms. Laser pulse with a longer wavelength interacts more strongly with the plasma plume and produces a large number of ions (also breakdown of air may occur), resulting in high plasma temperature and a strong continuum background radiation. For the analysis of paper samples it seems that it is best to use a laser which produces pulses from 1 to 10 ns of duration in the UV spectral region. From the practical point of view an essential feature of the laser is pulse-to-pulse stability. Corrections can be done by continually monitoring the pulse energy, but an unstable laser produces craters of variable size.

The goal of the optimization of the LIPS method for analyzing the spatial distribution of elements in the material is to minimize the mass removal and to maximize the emission intensity of spectral lines (signal-to-background ratio) without losing good signal-to-noise ratio. In practice it means that the excitation energy has to be kept as low, and the irradiance as high, as possible. Typically only a few nanograms of sample is ablated by each laser pulse. For analyzing such a small amounts of material the delay between the laser pulse and the detection has to be short, i.e. less than 100 ns, because the emission of plasma decays rapidly owing to the cooling of the plasma. This poses a problem in the timing of the detection system since in this case delay triggering from a light pulse is impossible. In order to synchronize the laser and the detection either a delay generator is triggered from the syncout of the laser or the laser is triggered by the delay generator. The success of this procedure depends on the jitter of the laser used. In this work triggering was mainly obtained from a light pulse of the laser resulting in a delay longer than 100 ns with respect to the laser pulse. Because the laser parameters vary from time to time and even more from one laboratory to an other reference samples are needed to verify the results obtained under different experimental conditions.

Matrix effects

LIPS-measurement is subject to matrix effects, i.e. the environment of the studied element has an effect on its emission intensity. Varying emission intensities for the same concentration of an element will be obtained in paper samples depending on I) the other compounds present, II) the particle size distribution, and III) the surrounding gas and its pressure in the plasma region. Each sample set has to be calibrated because of the matrix effects to obtain quantitative results. The matrix effect caused by the particle size is demonstrated with a set of samples where the coating pigment was kaolin. Particle size distribution of kaolins were 98% and 80% of particles less than 2 μm in size for kaolins A and B, respectively. Other parameters in this study were binder concentration (11 and 20 pph of SB-latex), coat weight (7 g/m^2 and 10 g/m^2) and calendering. LIPS intensity of silicon, originating from kaolin, was measured.

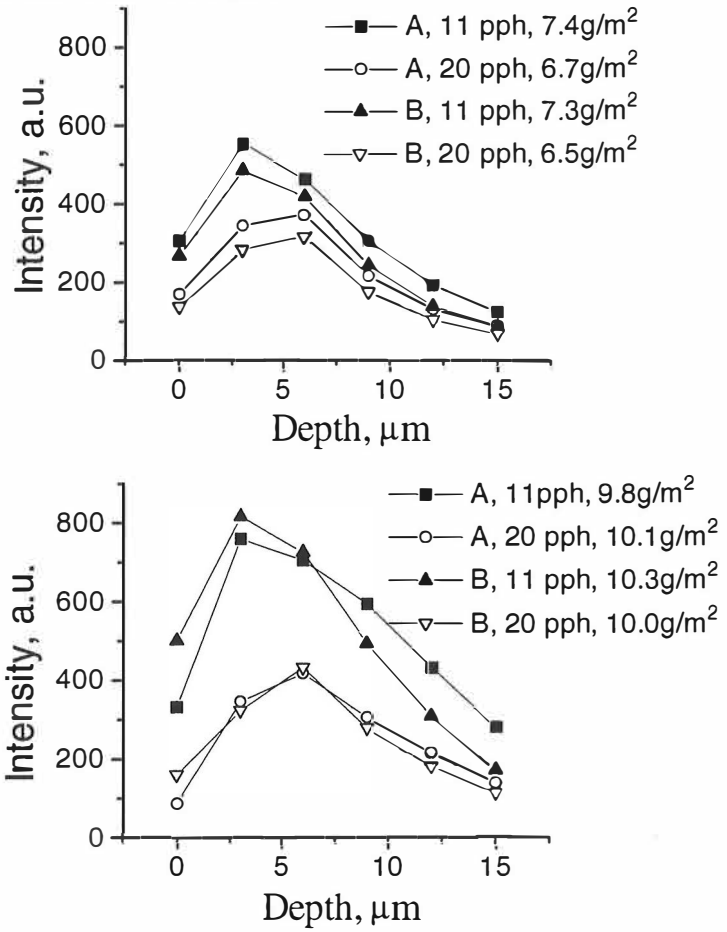

Figure 5.2. Effect of particle size and amount of binder on LIPS-intensity in calendered papers. A and B refer to fine and coarse average particle size, respectively.

As the average particle size of the pigment decreases the porosity becomes smaller, and the specific surface area increases. This means that more adhesive is needed to bind pigments together. In coatings with fine pigment the laser pulse interacts with a large area of pigment surface. The fine pigment particles are covered by a thinner layer of binder than the coarse particles. The samples with coat weight of 7 g/m^2 resulted in greater emission intensity in samples with finer pigments compared to samples with coarse pigments. The same effect was observed in papers with a coat weight of 10 g/m^2. However, in these samples the intensity on the surface was lower in fine particle samples (Fig.5.2). This may be due to the higher binder content on the surface caused by binder migration towards the surface. The calendering seems to reduce the LIPS-signal, which could be explained by the reduced area of coating surface and by more close packing of the pigment particles in the coating surface, that may contribute to decreased laser-material interaction. The LIPS-signal intensity is higher for10 g/m^2 coat weight papers because of better coating coverage than that of 7 g/m^2 papers. The increase of the binder concentration reduces the emission from pigments because there is less pigment in the ablated volume. It is difficult to compare two samples on the basis of results obtained by LIPS without knowing the formulation of coating colors.

It may be possible to utilize the matrix effects to evaluate the porosity of paper surface. Some indication of correlation between the intensity of LIPS-signal and the porosity of paper have been observed in preliminary studies. This subject needs further work.

Effect of the surrounding athmosphere

The effect of the surrounding athmosphere was studied by flowing argon or air over the measuring site. The plasma cools down more slowly in argon than in air. The intensity of the LIPS-spectrum in the background region measured in argon flow was approximately two times higher than that in air (Fig. 5.3A). The effect of buffer gas is clearly seen in the resonance line of Ca at 422.6 nm. The intensity of the line is reduced in air because of self-absorption but the self-absorption disappears in an argon athmosphere. The intensity in the center of the calcium line is eight times higher in argon than in air. This line is the most intense calcium line observed in the LIPS-spectrum and it may be used for measuring the filler distribution in paper. If this line is used for analytical purposes the argon buffering is recommended or otherwise the intensity should be measured from the broadened wing of the emission line instead of the line center.

The effect of the buffer gas is also seen in ion emission lines of Mg II doublet around 280 nm in Fig 5.3B. Due to faster cooling of plasma in air than in argon the intensity of the mg II line has diminished the decay times of the emission lines vs. the decay time of background continuum. The intensity ratio of emission lines measured in argon and in air, respectively, is greater for lines with a shorter decay time. In the present case Mg II ion lines decay faster than neutral lines at 285nm and 288 nm in the spectrum of Fig 5.3B.

Reason for disappearance of self absorption of calcium resonance line in an argon athmosphere has been assigned to metastable states of argon serving as a reservoir of energy[28]. When a ground state calcium atom collides with a metastable argon it is re-excited. The layer of ground state calcium atoms is not formed in the plasma plume in argon athmosphere. Possible re-excitation reactions are

$$Ar^m + Ca \rightarrow Ar + Ca^{+*} + e \qquad 5.1$$

$$Ar^m + Ca \rightarrow Ar + Ca^{*} \qquad 5.2$$

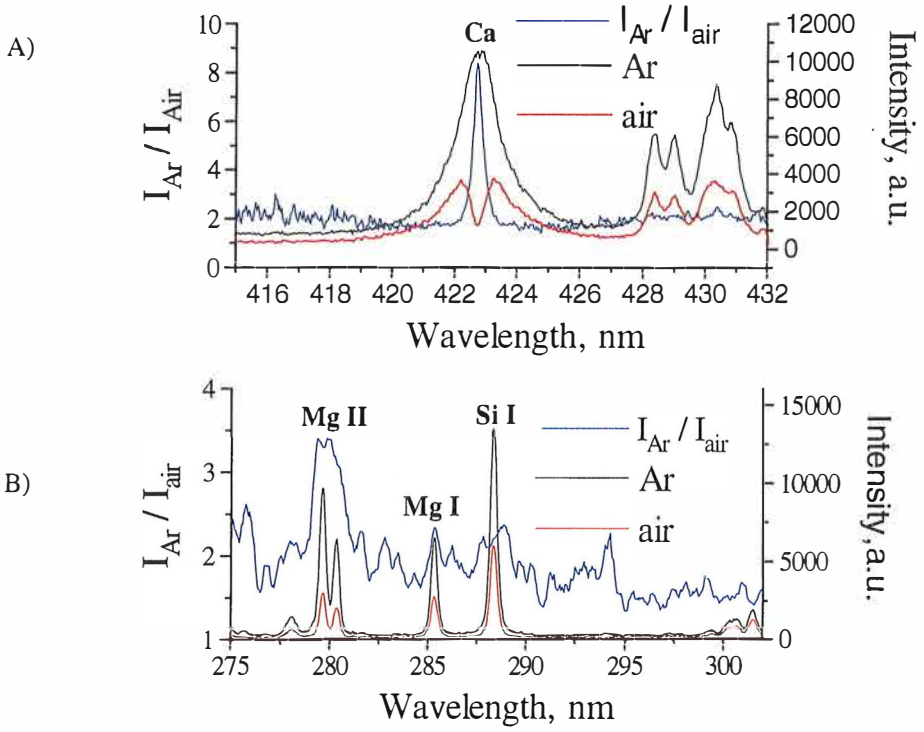

Figure 5.3. Effect of the surrounding athmosphere on the LIPS-spectra.

Calibration

Because of matrix effects every sample set has to be calibrated. Often only one sample, in which the coat weight is only approximately known, is available. In most cases linear dependence is observed between the LIPS-signal and the coat weight (Fig 5.4). The effect of filler is normally weak which means that the conversion of measured intensities to coat weight values becomes possible . If one has a set of samples available then the contribution of fillers in the signal can also be evaluated.

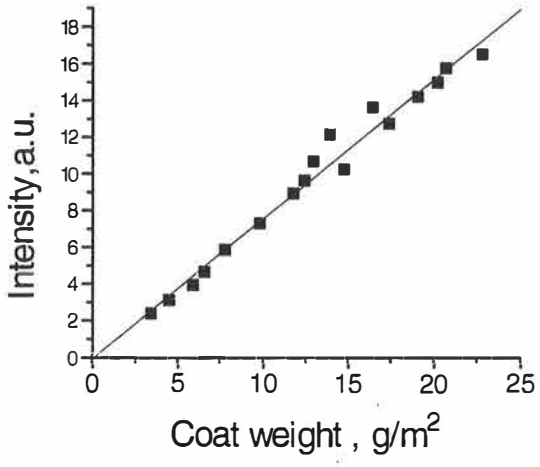

Figure 5.4. Calibration curve of LIPS intensity vs. coat weight.

In multilayer coatings each coating should be calibrated separately. Otherwise the interpretation of the result is only qualitative. If the coating layers have different intensity/coat weight response it is hard to evaluate the total coat weight by directly measuring all coatings. The same emission intensities may be obtained though the relative compositions of the coatings vary from pure layer I to pure layer II as illustrated in Fig 5.5.

The intensities measured from different layers should be treated separately. This is possible in the LIPS-measurement if the coating layers give different relative intensities of the observed emission lines.

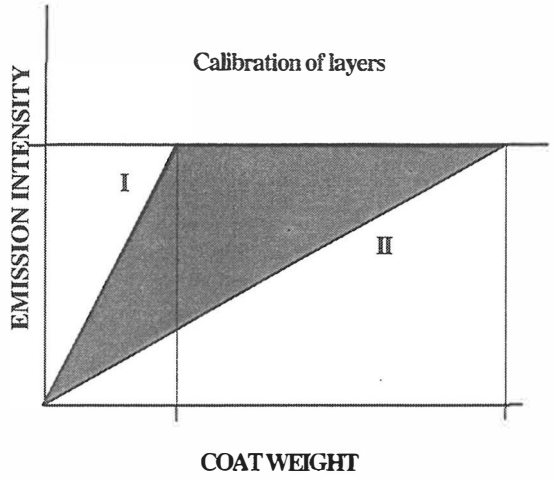

Figure 5.5. Schematic presentation of calibration of a double coating. Coatings differ with response in intensity from each layer. Emission intensity is a vector sum of the two calibrations.

Correction of temperature variation of plasma

Temperature of plasma varies from pulse-to-pulse due to variation in laser energy and/or the different composition of elements in plasma. The energy fluctuation of the laser should be accounted for. LIPS-intensity is linearly dependent on laser energy in the energy range used in this work. Continuous monitoring of laser energy from pulse-to-pulse can be used to solve this problem. To obtain corrections the intensity dependence of the emission lines in question are plotted against the pulse energy. The slope of the plot is the correction coefficient for energy variation.

Another approach is to use Mg(I)/Mg(II) line intensity ratio as a measure of the relative temperature of plasma. As plasma cools each emission line decays at a rate characteristic to the transition and plasma temperature (Fig.5.6). Often one is interested in measuring - e.g. the Si/Ca ratio - in order to distinguish between different coating layers. The silicon calcium intensity ratio depends on temperature. Temperature variation can be accounted for by using the Mg I and Mg II intensity ratio, as shown in Fig.5.7. To obtain calibration curve in Fig 5.7, the intensity ratios of the needed emission lines are read at fixed delays from the decay curves shown in Fig 5.6. This demonstrates that at different plasma temperatures the intensity ratio shows a linear dependence.

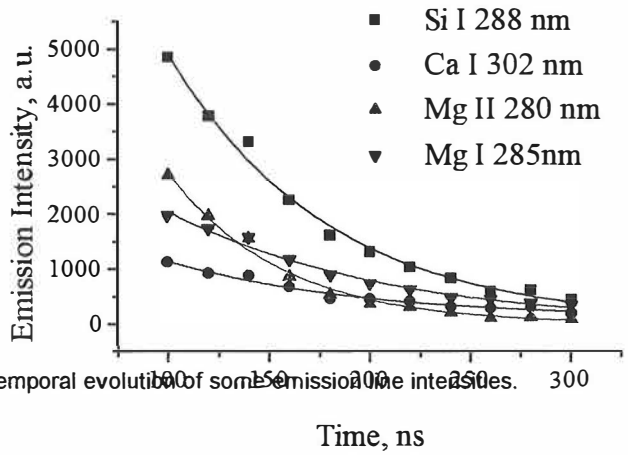

Figure 5.6. Temporal evolution of some emission line intensities.

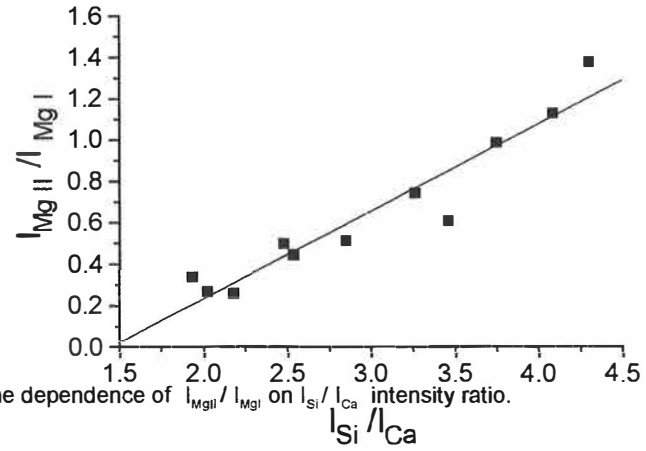

Figure 5.7. The dependence of I_{MgII} / I_{MgI} on I_{Si} / I_{Ca} intensity ratio.

Craters

Laser ablation is especially useful in the analysis of multilayer coatings layer by layer. Once the material is ablated and a crater is formed it is possible to examine the dimensions of the crater by using a microscope. The bottom of the crater contains information about the structure of the bulk material. The craters can be analyzed by surface analysis methods like ESCA, ATR-IR and SEM-EDX to get information from compounds in the coating. Exact dimensions of craters can be obtained by using atom force microscopy (AFM). The AMF picture of a crater produced by a single laser pulse is shown in Fig 5.8. The dimensions of the crater are 30 μm in diameter and 2 μm in depth.

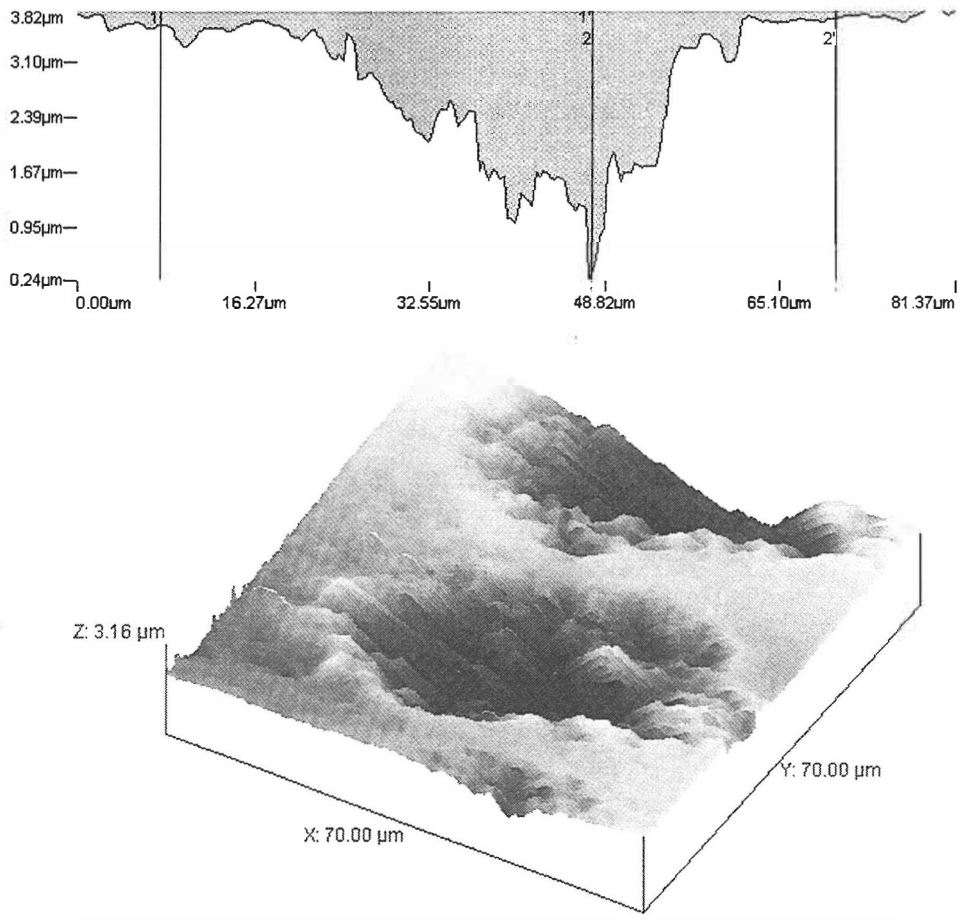

Figure 5.8. An atom force microscope picture of a crater produced by a single laser pulse in coated paper and the cross section of the crater (top).

The coating can be peeled off by consecutive ablation of the same position. Microscope pictures of craters created by vaporizing the coating material by varying number of pulses (1, 2, 4, and 8 pulses) is shown in Fig. 5.9. In this case eight pulses are needed to remove all coating. This technique can be utilized in the microscopic analysis of coating structure. In our LIPS measurements the microscopic study of craters has been used for the evaluation of the effective diameter of the laser focus on the sample surface.

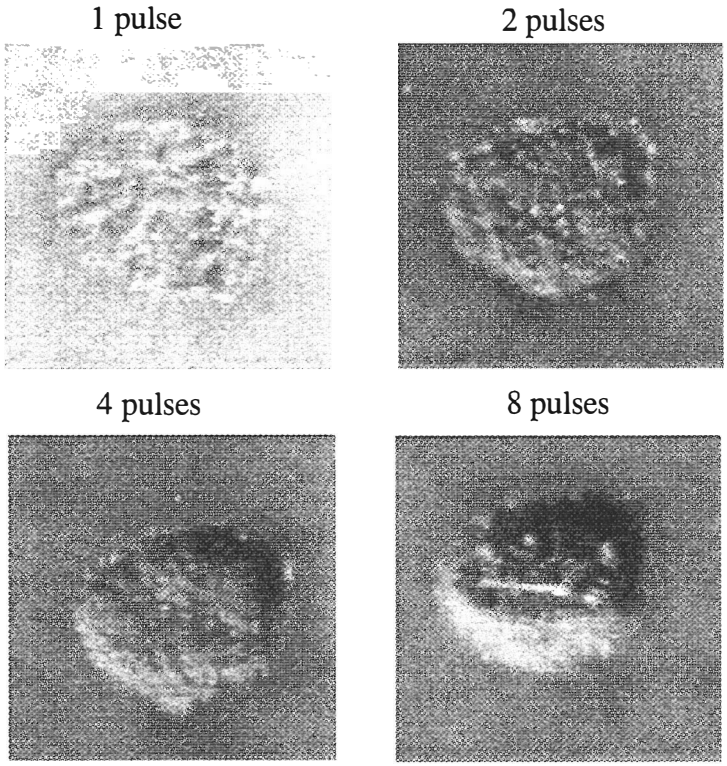

Figure 5.9. Optical microscope pictures of craters produced by a varying number of laser pulses.

5.2 APPLICATIONS OF LIPS-METHOD IN PAPER ANALYSIS

The original aim of this work was to develop a method for measuring the coat weight distribution in coated paper. The work was later extended to the study of distributions of individual material components in the coating and in the base sheet. In the following these issues are discussed.

5.2.1 QUALITATIVE ANALYSIS OF PIGMENTS

The pigments commonly used in paper coatings are kaolin, calcium carbonate and to a lesser extent talc and titanium dioxide. The pigment composition of a coating can be analyzed in a few minutes by using the LIPS-method. The relative line intensities of the elemental spectrum are characteristic for each pigment. LIPS spectrum of a coated paper sample with mixed kaolin and calcium carbonate coating is shown in Fig 5.10. The most intense lines are labeled with element symbols.

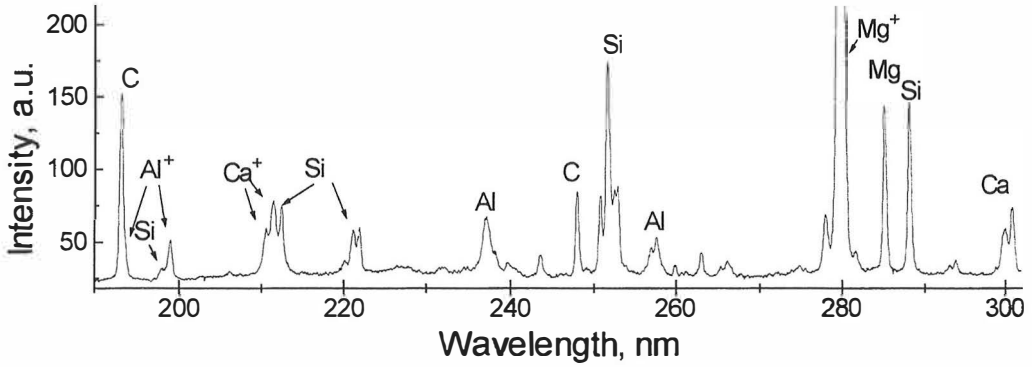

Figure 5.10. LIPS spectrum of coated paper.

The emission lines of calcium originate from calcium carbonate, and the aluminum and silicon lines are from kaolin. Carbon lines at193 nm and at 247 nm are from $CaCO_3$ and the organic compounds of the coating. In the spectrum above magnesium is an impurity which originates from both pigments used in the coating. The magnesium lines at 280 nm and 285 are very sensitive indicators of even minor amounts of Mg in the coatings. For qualitative analysis of pigment composition Mg emission the line at 202.6 nm is recommended shown in the spectrum

of talc in Fig 5.11. For the analysis of LIPS spectrum it is helpful to have spectra of raw materials used to make the coating for comparison.

The origin of a pigment can be traced back in some cases due to the mineral impurities like Mg, Ti, K. For example, kaolin of British origin contains potassium and kaolin from the USA contains titanium as an impurity. Brazilian kaolin does not contain detectable amounts of magnesium which is the case in kaolins from other origins.

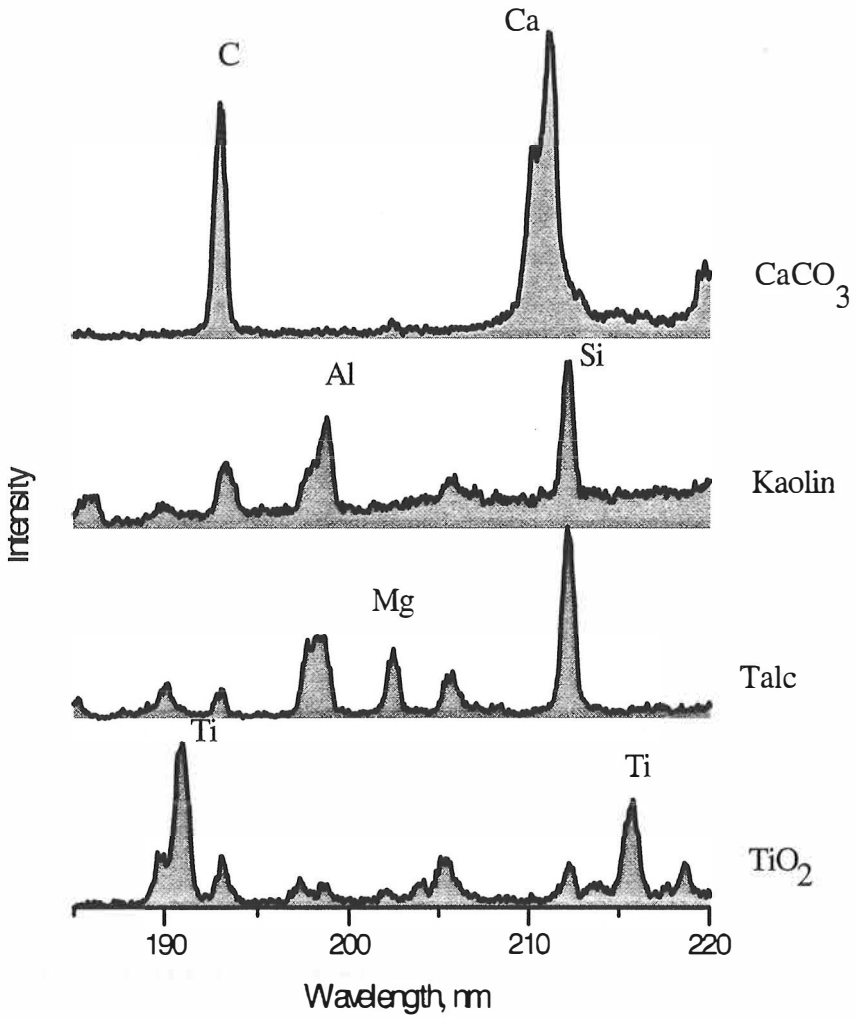

Figure 5.11. Spectra of coating pigments;kaolin, calcium carbonate , talc and titanium dioxine.

Spectra of kaolin, calcium carbonate, talc, and TiO_2 are shown in Fig 5.11. The wavelength range from 185-215 nm has turned out to be the best choice for analysis of coatings because all relevant elements show useful emission lines in this wavelength range. The increase of background in the spectrum of kaolin is due to aluminum. When increased sensitivity is needed then other parts of the spectrum may be used. For instance, the wavelength region 275-302 nm is useful for the analysis of kaolin and calcium carbonate ratio in multilayer coatings. The best emission line for the analysis of filler distribution is the calcium line at 422.6 nm.

5.2.2 COAT WEIGHT

In the coat weight studies a sufficient number of laser pulses has to be used to remove the entire coating layer. For each sample set the number of pulses needed for removal has to be determined separately. The measured integrated intensities of the emission lines of a pigment at each xy-position are converted to the coat weight by using a calibration.

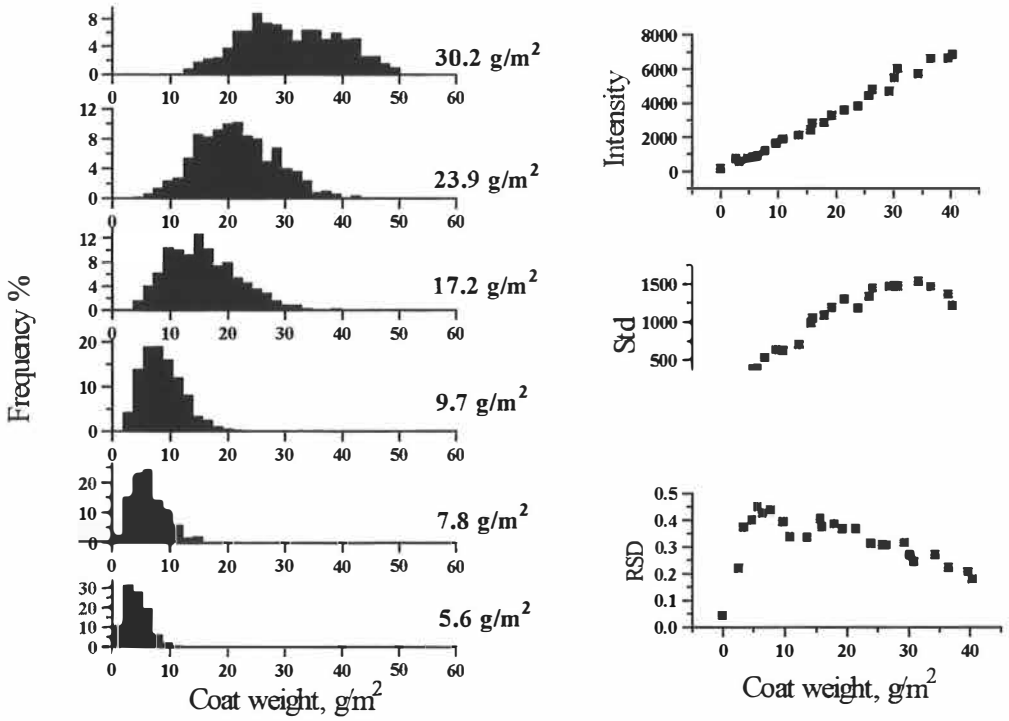

Figure 5.12. LIPS intensity, standard deviation, relative standard deviation (right), and the frequency distribution of intensities (left) as a function of coat weight.

There are several ways to represent the results. A commonly used way is to give the average coat weight ± standard deviation. Representations in the form of graphs are often more informative. One such way is to present coat weight distribution as histograms (Fig 5.12. left). The shape of the histogram shows the type of coating. A narrow and symmetric histogram represents contour coating, i.e., the thickness of coating is even and it follows the shape of the base paper surface. Histograms of coat weights 17.2 g/m^2 and 5.6 g/m^2 in Fig 5.12 represent good and bad coating coverage, respectively. The purpose of coating is to fill the voids of the base paper with a smooth and porous coating layer. The microscopic spatial variation of coat weight increases as the coat weight is increased towards full coverage of the base paper. Full coating coverage is usually obtained at around 12 g/m^2. This can be seen in histograms as an absence of low coat weight scores. The relative standard deviation (RSD) of integrated intensity experiences a turning point at full coating coverage (Fig. 5.12 right, bottom).

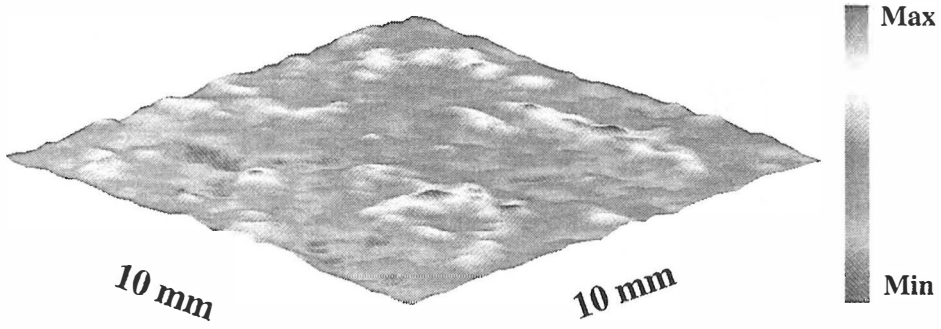

Figure 5.13. Coat weight distribution map of LWC paper.

Coat weights can be measured from a desired area and represented as a coat weight distribution map (Fig. 5.13). The properties of coated paper can then be analyzed more precisely by means of image analysis. This was not included in the present study.

Coating coverage

A special case of coat weight distribution is the degree of coating coverage (DCC). In this work coating coverage is defined as an average thickness of coating of 2 μm thick surface. DCC is evaluated by using the intensities of the first two ablated layers. To obtain DCC the average intensity of the first layer I_{ave} is divided by the average intensity of the full coating I_{full}. I_{full} is defined as average of intensities in locations of the first layer where a second pulse gives an obvious signal.

$$DCC\ \% = 100*I_{ave}/I_{full} \qquad 5.3$$

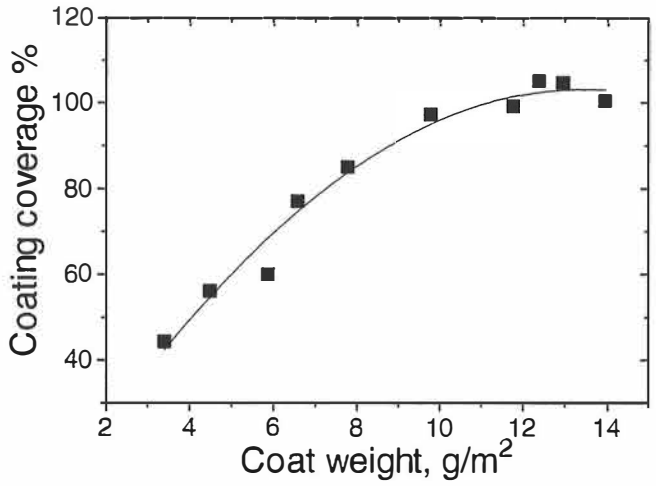

Figure 5.14. Coating coverage of LWC paper as a function of coat weight.

Coating coverages for a series of LWC papers as a function of coat weight are shown in Fig.5.14. The full coverage is obtained at coat weight of 12 g/m^2. Measurement of coating coverage may be utilized in quality control and in the research and development of paper coatings to find optimum coating color and running parameters for a coating.

Multilayer coatings

High quality printing papers have often several coating layers. The coat weight analysis of the total coat weight is not always adequate to solve the quality problems related to coat weight variations in these grades. The coat weight of the top coating may vary more than the total coatweight and this may give rise to quality problems. Measurement of multilayer coating by LIPS is similar to the measurement of a single coating, only the data handling is different.

The response of the signal for each coating layer has to be known for the evaluation of absolute coat weight values. The qualitative picture of coating layers is obtained without calibration. In the coat weight measurement of double coatings one has to know the relative signal response of both layers. The layers may be analyzed reliably if they have different pigment contents.

A typical case is that two coating layers have kaolin and calcium in different compositions in each layer. For instance the pigment in pre-coating may have a larger average particle size giving rise to lower signal levels than coating with smaller particles.

Case: double coated MWC papers

Coat weight distributions of two double coated MWC paper samples were studied. Papers were characterized by visual inspection as good and bad by the papermaker. LIPS analysis was performed in the machine direction on the top side of the paper along a length of 25.6 mm at 0.1 mm steps. Silicon and calcium intensities were measured as indicative of concentrations of kaolin and calcium carbonate, respectively. Relative kaolin content was evaluated from the ratio $I_{si}/(I_{si}+ I_{Ca})$.

The distribution of relative kaolin content in the xz-plain of paper samples are shown in Fig 5.15. A previously determined calibration (different recipe) was used to evaluate the pigment content in the two coatings. In these samples the kaolin/$CaCO_3$ ratio was 50/50 in the top coating and 15/85 in the pre-coating. The frequency distribution of relative kaolin content in ten layers is shown in histograms of Fig.5.17. It should be noted that filler may make a small contribution to signals from pre coating.

In this case the relative kaolin content of 30 pph was used as a criterion to separate the two coating layers (Fig.5.16). Top coating (red color) is the area above 30 pph and pre-coating (yellow) is the area where relative kaolin content is below 30 pph. When the intensity of I_{Si}+ I_{Ca} of a sampling point is below 10 % of the maximum value, the location is considered as base paper (blue). The top coating is more evenly distributed in the sample classified as good and it does not penetrate as deep as in the bad sample. In a good sample the pre-coating forms a layer that has better coating coverage.

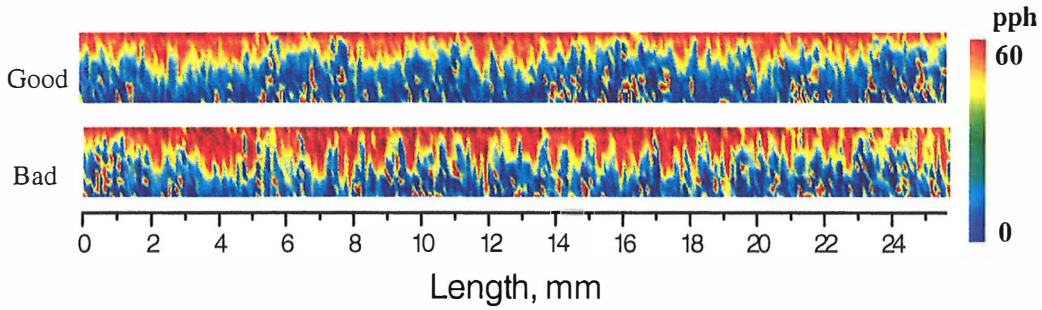

Figure 5.15. Distribution of kaolin content in paper samples. Thickness shown is about 25 µm.

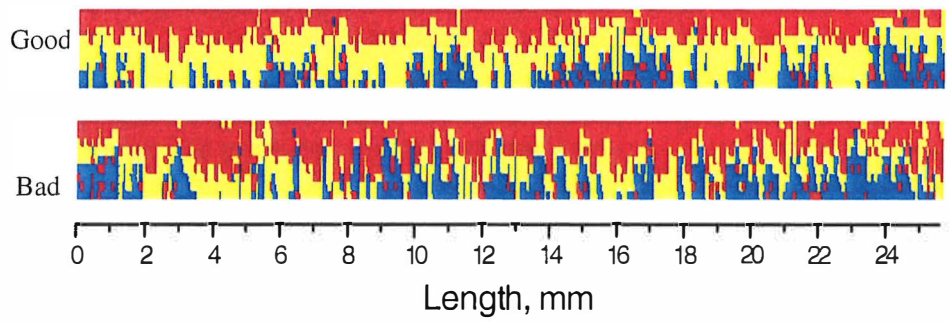

Figure 5.16. Distribution of coatings. Top coating (red), pre-coating (yellow), base paper (blue). Red dots in base paper region represents filler.

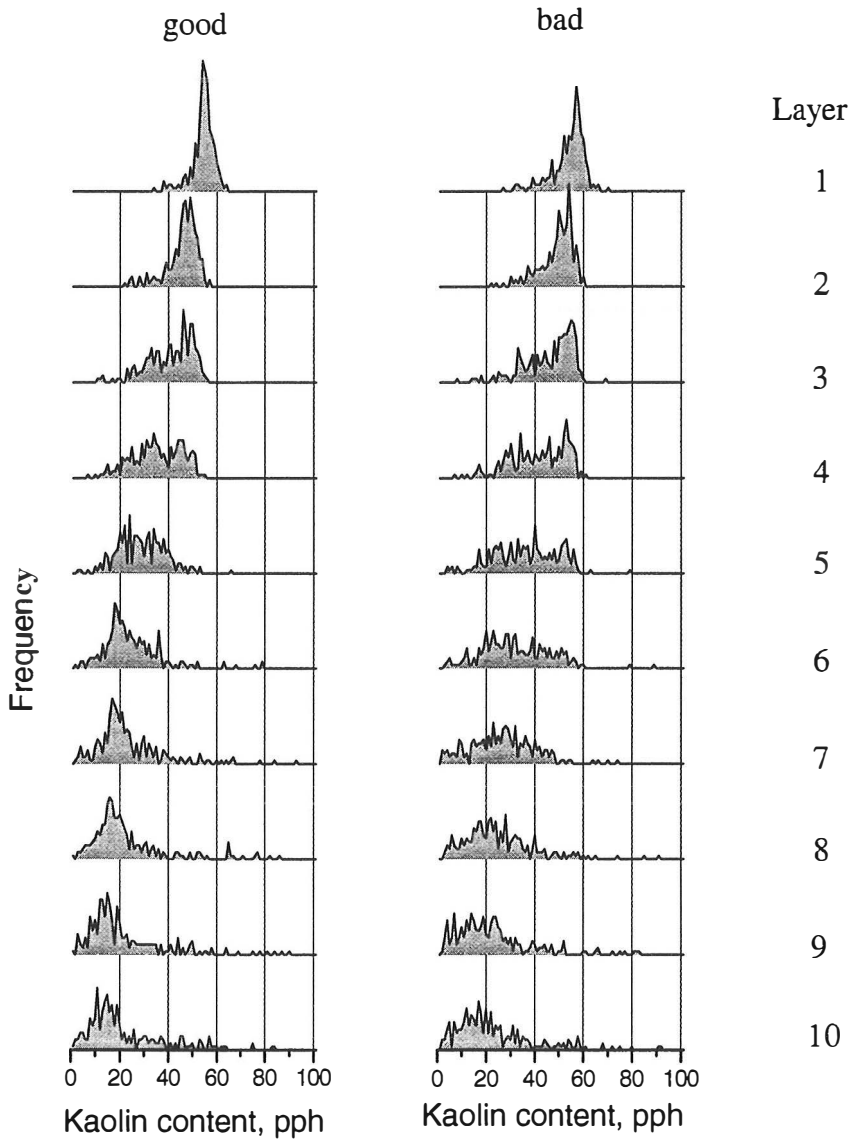

Figure 5.17. Frequency distribution of parts of kaolin in MWC paper samples as a function of depth. One layer is about 2-3 µm thick.

As an example of high quality paper with multilayer coating the coat weight distribution is presented in Fig 5.18. The pre-coating has filled in the voids and covered the base paper giving an almost smooth surface. The top coating (red layer) forms a nearly even coating layer on the top of the pre-coating (yellow layer).

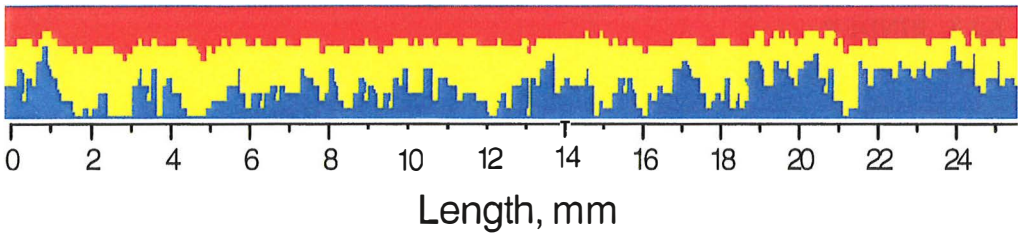

Figure 5.18 Distribution of coatings Top coating (red), pre-coating (yellow), base paper (blue). Thickness shown is about 30 μm.

As a further demonstration of the efficiency of the LIPS technique in analyzing multiply coated papers, results of 3-dimensional distributions of coating layers are shown in Fig.5.19. Distribution of coatings in eight consecutive layers (2-3 μm thick) of 1 cm^2 area were studied. Red color refers to top coating, green color to pre-coating and blue color represents base paper. The interface of the coating layers is seen in the forth layer at a depth of about 10 μm.

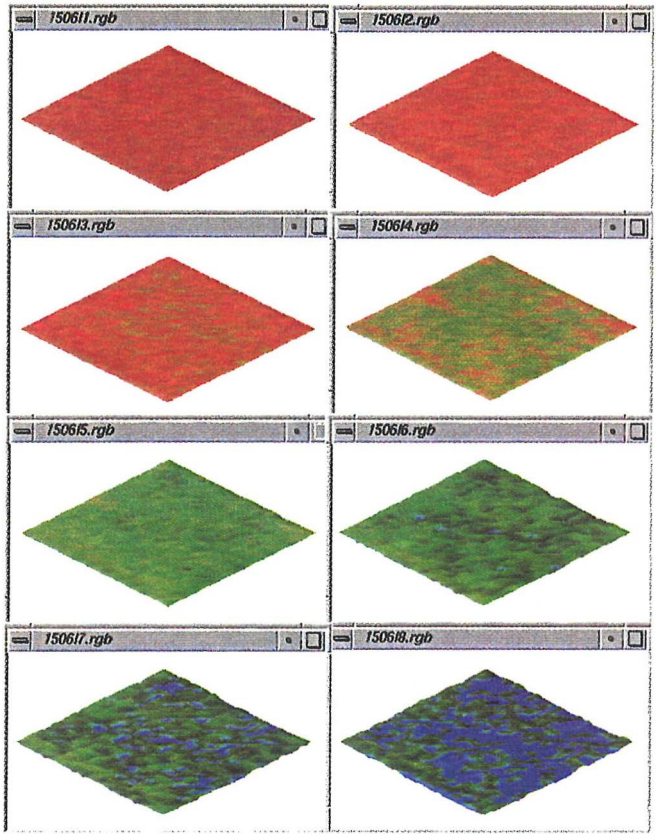

Figure 5.19. Distribution of coating as a function of depth , top coating (red), pre-coating (green), base paper (blue).

5.2.3 BINDER

Binders added in coatings are organic polymers, mainly starch and latex. The binder content affects the LIPS-spectrum in two ways: it decreases the emission intensity of the pigment elements (calcium, silicon, aluminum) and on the other hand it increases carbon emission line intensities (Fig. 5.20). There are two detectable lines of carbon in the LIPS-spectrum, one at 193 nm and the other at 247 nm. The carbon line at 247 nm is not a suitable candidate for analysis because there are no Ca lines nearby. Such lines are needed to allow evaluation of the proportion of organic carbon from the total carbon signal of the coating. If a wider spectral range is covered this is done at the expense of spectral resolution. The best range for the analysis of binder content is between 190 and 220 nm hence all the relevant elements of paper have emission lines in this region. These include 193 nm for carbon, 211 nm for calcium, 213 nm for silicon, 206 nm for magnesium, and 190 nm for titanium (Fig. 5.11).

The binder/pigment ratio was studied by measuring the intensity ratio of carbon/elements of pigments (Si, Ca). Because the carbon emission is the sum of both organic and inorganic carbon these had to be separated. The inorganic carbon originates primarily from calcium carbonate and could be subtracted from the total carbon signal by using the scaled intensity of the nearby calcium line.

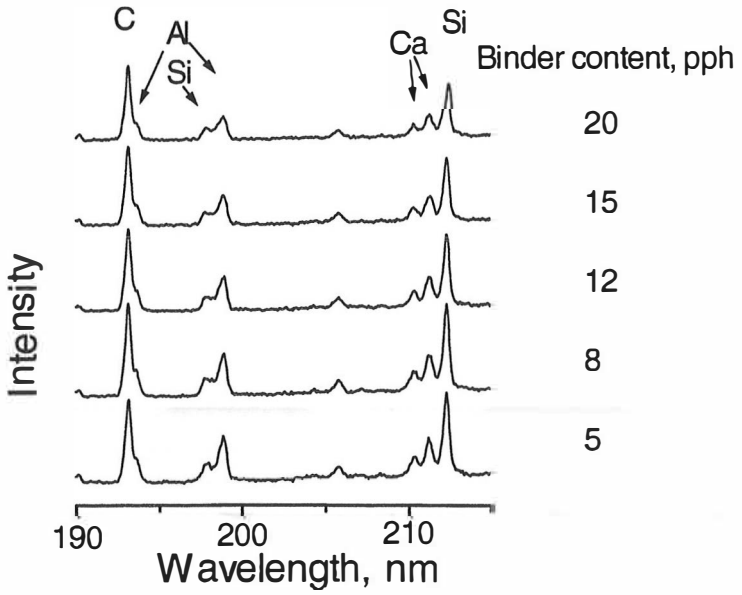

Figure 5.20. Spectra of coatings with different binder content.

The overlapping aluminum lines at 193 have a small effect on the intensity response of the carbon line at 193 nm. This can be subtracted by using other aluminum lines or silicon lines since both elements are constituents of kaolin.

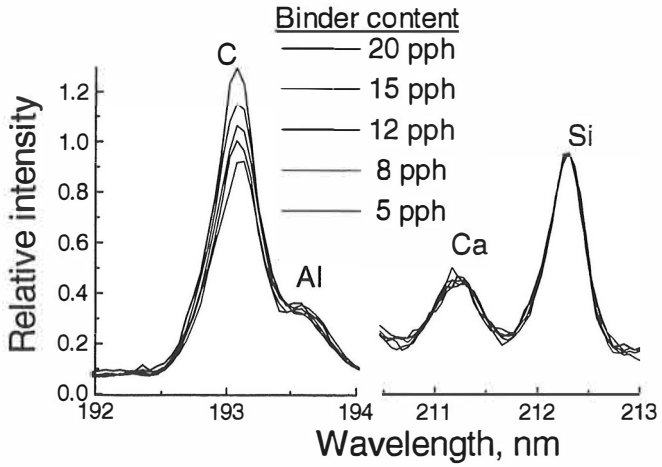

Figure 5.21. Normalized spectra of coating with different binder content. Spectra are normalized by using silicon line intensity at 212.3 nm.

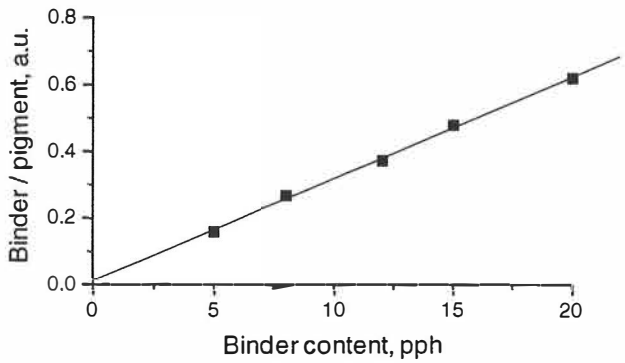

Figure 5.22. The intensity ratio of (organic carbon/pigments) as a function of binder content.

The possibilities for evaluating the binder content in paper coatings were studied in two cases. In the first case the coating contained 50/50 parts of kaolin and calcium carbonate, respectively. The binder content was varied between 5 pph and 20 pph. The intensity ratio binder/pigment was evaluated from

$$I_{C\_org} / (I_{Si} + I_{Ca}) \qquad 5.3$$

where

$$I_{C\_org} = I_C - a\, I_{Si} - b\, I_{Ca} \qquad 5.4$$

where a and b are coefficients measuring the proportion of kaolin and calcium carbonate line intensities to the carbon line intensity (I_C), respectively. The relative intensities of calcium and silicon lines were scaled to give equal intensities of pigment lines. The linear dependence of the intensity ratio as a function of the binder content is shown in Fig.5.22.

In the second case the binder content was kept constant and the pigment composition was varied (kaolin/$CaCO_3$ -ratio was 20/80, 50/50, 80/20, 100/0). Spectra of these coatings are shown in Fig.5.23. The base line increase is due to aluminum in samples with a high kaolin content. The intensities of emission lines are almost linearly dependent on kaolin content (Fig 5.24).

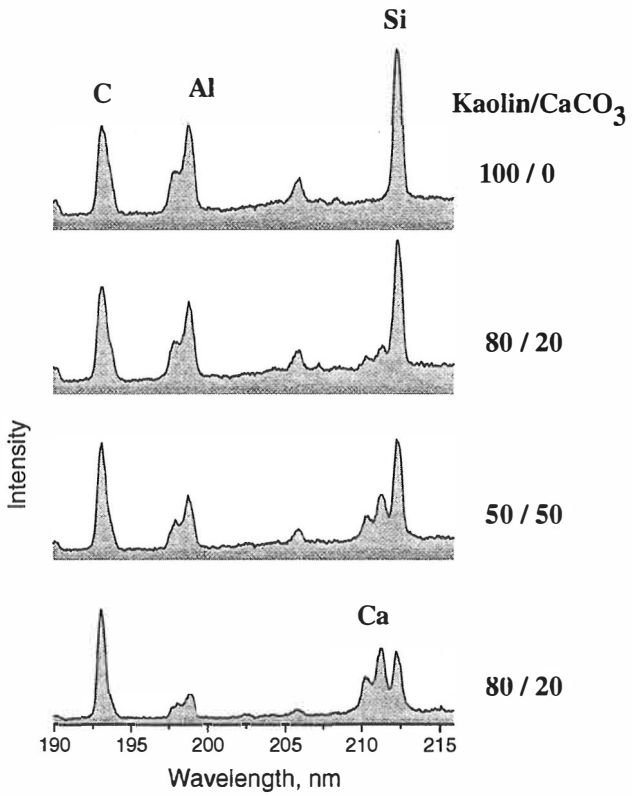

Figure 5.23 Spectra of coatings with different pigment mixture and constant binder content.

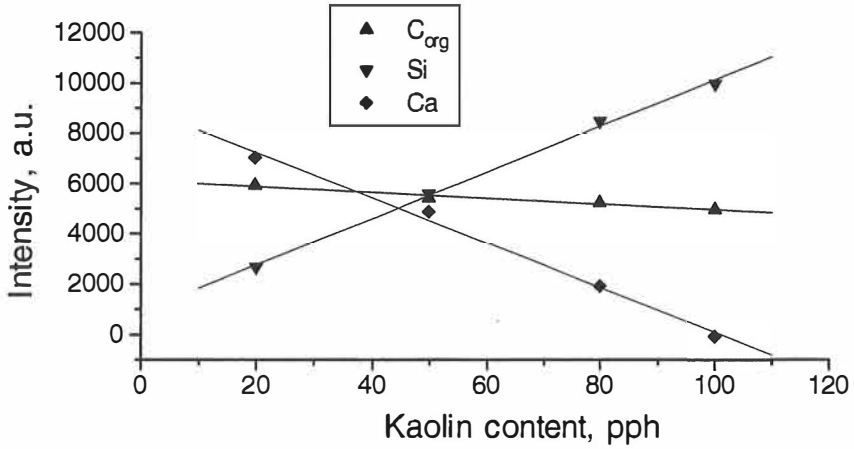

Figure 5.24. Intensities of emission lines as a function of kaolin content.

The intensity of C_{org} is slightly decreased as the kaolin content is increased. This is due to the decrease of plasma temperature as the kaolin content is increased, which was verified by measuring the Mg (II) /Mg (I) ratio as a function of kaolin content (Fig 5.25).

The calculated intensity ratios Si/(Si+Ca) and C_{org}/(Si+Ca+C_{org}) show that the silicon content is linearly dependent on kaolin content and the organic carbon content (binder) is almost constant (Fig.5.26). The deviations are due to the temperature variations of plasma induced by matrix effects.

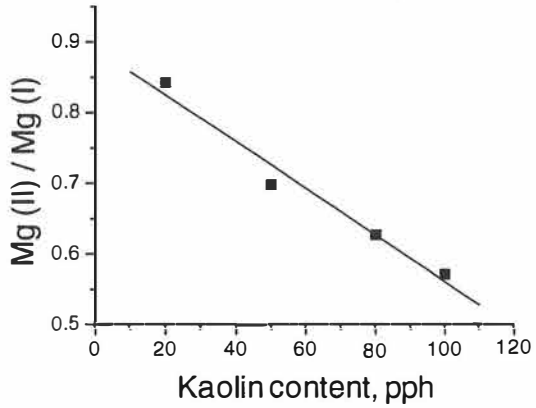

Figure 5.25. Effect of kaolin content on temperature of plasma.

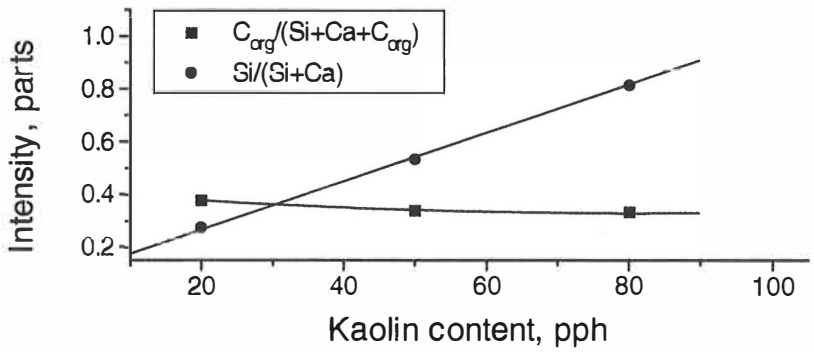

Figure 5.26. Relative organic carbon and silicon intensities as a function of kaolin content.

The spatial distribution of binder content was used to study printability. The relative standard deviation (RSD) of binder content (C/Si) was correlated to the visual evaluation of printed papers. The formulations of coating colors are presented in table 5.1. All coating recipes include 1 pph of CMC. Two coating weights 7 g/m^2 and 12 g/m^2 were studied. The visual evaluation of imprint in the trial print is correlated to RSD of binder content (Fig 5.27). The tendency for water mottling according to binder type decreases in the order starch, SB-latex, and PVAc. The distribution of binder was more even in the thicker coating (12 g/m^2).

Table 5.1. Sample specifications

Sample	Pigment	Binder	Base
kp 12,13	100 kaolin	10 SB-latex	LWC
kp 16,17	100 kaolin	8 SB-latex 8 starch	LWC
kp 20, 21	50 kaolin 50 $CaCO_3$	10 PVAc	LWC
kp 24, 25	30 kaolin 65 $CaCO_3$ 5 PS-pigment	10 SB-latex	Fine
kp 28, 29	30 kaolin 70 $CaCO_3$	10 SB-latex	Fine

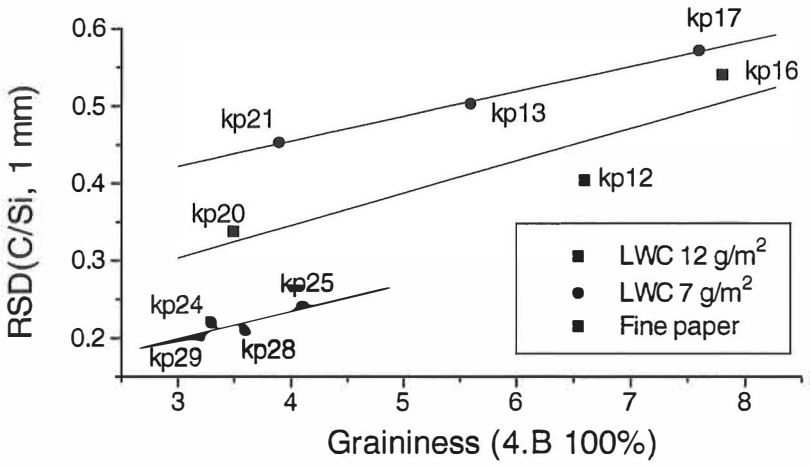

Figure 5.27. Relative standard deviation of binder content vs. graininess in print trial.

It is possible to distinguish adjacent coating layers also by looking at binder contents of layers as shown in Fig 5.28. Two paper samples with double coating were studied. In the first sample coating colors were 5 pph of binder in the top and 20 pph in the bottom layer. In the second sample the coatings were applied in reverse order. The binder content at the surface is much higher than in the bulk coating.

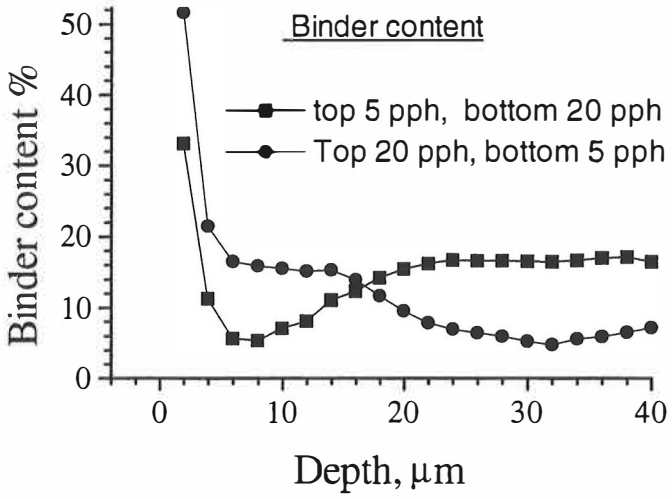

Figure 5.28. The depth profiles of binder concentrations of two double coated papers.

5.2.4 FILLER

Filler distributions were studied for copy paper, SC-paper and for base papers of coated grades. In the measurements the matrix effects had to be considered, i.e. the type of filler and the amount of adhesives in the base paper affect the intensities of LIPS signals.

Typical paper thickness is about 100 μm. The focusing parameters for LIPS-analysis of fillers should be chosen to keep the diameter of the laser focus constant through the paper thickness. The spot size has to be sufficiently wide to create plasma large enough to be seen by the detection system. Walls of deep and narrow craters may provide screening for optical access to the plasma. The most commonly used fillers are kaolin and calcium carbonate. In the present experiments the distribution of calcium carbonate in base paper was studied. The neutral calcium atomic emission line of calcium at 422.6 nm was monitored. This resonance line is the most intensive calcium line. This line may suffer from self-absorption if the concentration of calcium in the sample is too high. A possibility of self-absorption may be avoided by argon buffering (see p. 27).

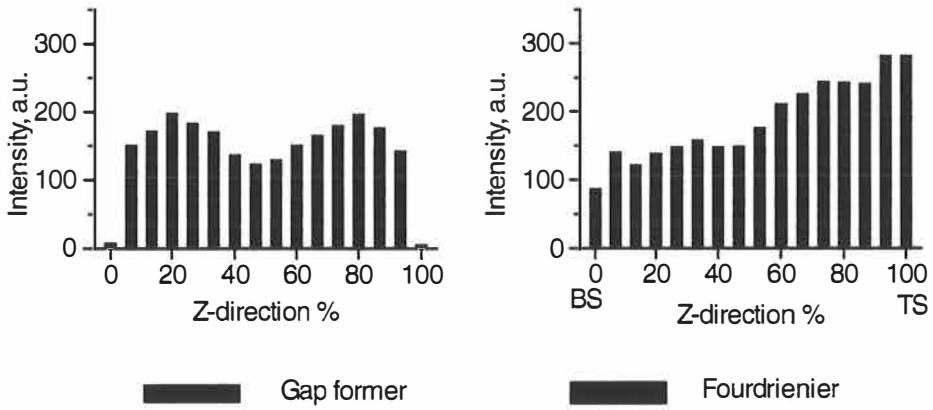

Figure 5.29. Distribution of filler in paper made by gap former and fourdrienier.

Filler distributions were measured in the same way as pigment distributions in coatings. To obtain a LIPS signal from fillers a larger measuring area than 0.2 mm in diameter and a more energetic laser pulse had to be applied. This is because pigments are less densely distributed in

bulk paper than in paper coatings. Measurements were carried out from the surface towards the center of base paper from both sides of the paper.

The results can be visualized in various ways, the most convenient being the z-directional profile of filler content (Fig. 5.29). The shape of the profile depends primarily on the former used to make the paper. Fourdrienier is a single wire machine where dewatering occurs mainly through the wire. The filler content in papers decreases from the top side towards the wire side. In the gap former there are two wires and dewatering is to both directions. A paper made with a gap former has a filler poor region in the center of paper and there is very low filler concentration on the surfaces. It was thought that sizing could cause a smaller LIPS signal from the surface but no difference was observed, only the signal level is higher in the interior of paper in unsized paper (Fig. 5.30). One possible explanation for a low signal from the surface is that fillers are rinsed due to effective dewatering.

The spatial distribution of calcium in the xz-direction is shown in Fig. 5.31. It seems that the fillers form concentrated areas in paper. Filler distribution may have an effect on the quality of gloss in coated papers after calendering. Correlation between the filler distribution and quality of coated paper was observed. This is a topic that needs further study.

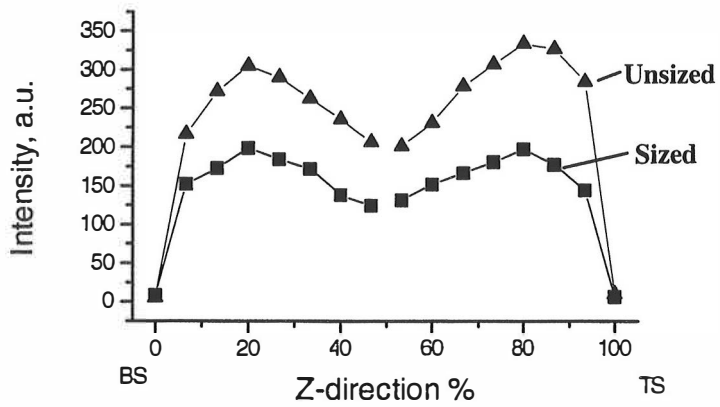

Figure 5.30. Effect of sizing on the intensity of calcium line in z-direction distribution of fillers.

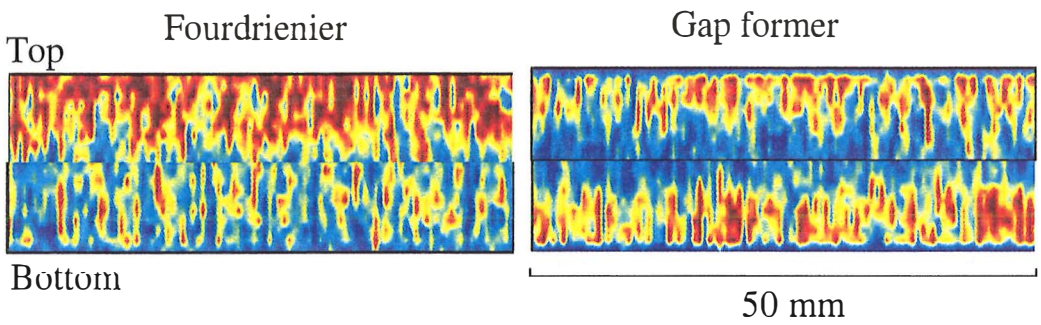

Figure 5.31. XZ-direction distribution of fillers in papers made by gap former and fourdrienier. Measurements were carried out from the surface towards the center of the paper. Top and bottom side measurements are from a different region of the same paper sheet.

The spatial distribution of fillers can be analyzed in 3 dimensions. The resolution in x- and y-directions is of the order of 0.2 mm and in z-direction from 5 to 10 μm. Filler distribution can be visualized as xy-intensity maps such as shown in Fig 5.32.

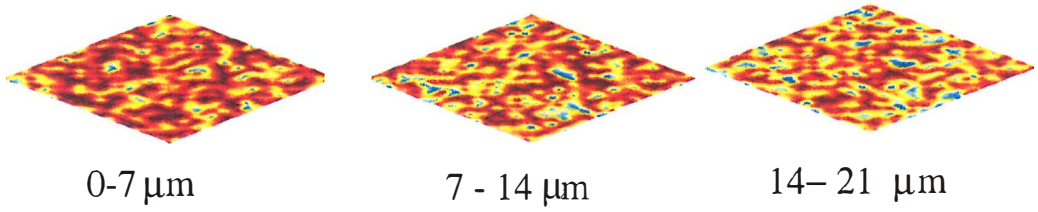

Figure 5.32. XY-direction distribution of fillers in three consecutive layers. The analysis was started from top side of the paper.

Three dimensional distribution of fillers in paper can be obtained by LIPS in a short time, i.e. 1000 points from one side may be recorded in half an hour. LIPS measurement could be used for measurements of filler distributions in quality control laboratories of paper mills.

5.3 LASER-INDUCED FLUORESCENCE

This work was initiated with the analysis of coat weight distribution of paper by laser-induced fluorescence (LIF). The fluorescence was generated by focusing a pulsed laser beam (308 nm, 15 ns) onto the paper surface with a focal area of 0.1 mm in diameter. Irradiance of the laser pulse on the sample was ~10^6 W/cm^2, two orders of magnitude lower than used in the LIPS-measurements. The fluorescence intensity was integrated between wavelengths from 400 nm to 500 nm. The advantage of using laser excitation instead of lamp excitation in the study of coated paper is that the intense laser pulse can penetrate through the coating. The fluorescence efficiency of materials used in paper making decreases in the following order: FWAs >> binders, fibers >> pigments. Coat weight distribution of paper can be analyzed by LIF if the fluorescent whitening agent (FWA) is added either in the coating or in the base paper. The most often used FWAs in the paper industry are the diamino stilbene derivatives (the diacyl, diacyl sulfamide and triazinyl are the most common). If FWA is added in the coating the fluorescence intensity from the coating increases. On the other hand, if FWA is added in the base sheet fluorescence intensity decreases as the coating with no FWAs will screen the excited emission from the base paper. A fluorescence image of the coat weight distribution of a paper board sample is shown in Fig. 5.33. A total of 10 000 spectra was measured from a sample area of 1 cm^2.

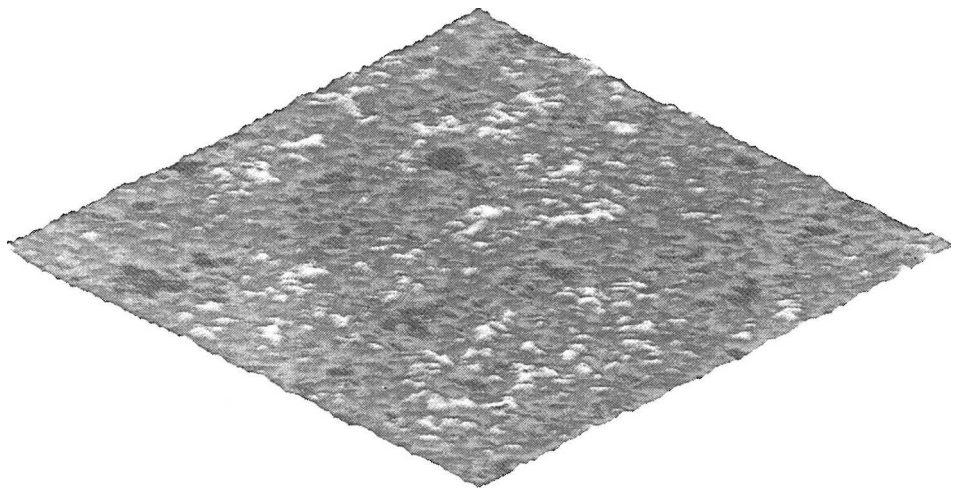

Figure 5.33. Fluorescence image of coated paper board. Measurement area is 1 cm^2 with 0.1 mm sampling interval.

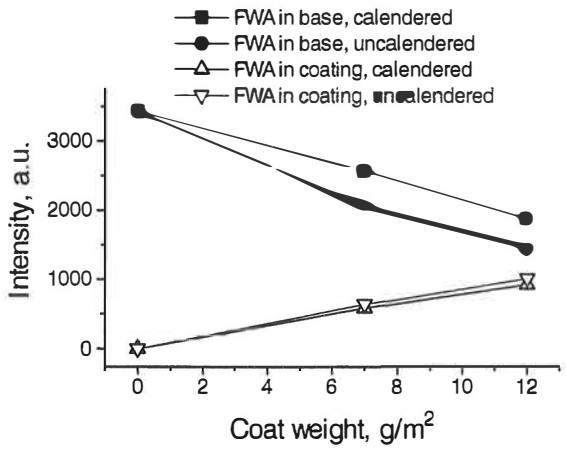

Figure 5.34. Fluorescence intensity as a function of coat weight in calendered and uncalendered papers. Fluorescence whitening agent is added either in the coating or in the base paper.

The dependence of fluorescence intensity on coat weight is almost linear for coat weights up to 12 g/m^2 (Fig. 5.34). At higher coating weights fluorescence intensity will approach asymptotically to the constant level characteristic of infinitely thick coating layer. The coat weight range that can be analyzed is dependent on the energy of the laser pulse, i.e. the more powerful the laser pulse the wider the linear signal range. Fluorescence excitation of coating is more effective in uncalendered papers than in calendered papers. This can be seen in fluorescence intensities. For the paper grades where the FWA is present in the base paper the intensity is lower in uncalendered than in calendered paper. On the other hand if the FWA is in the coating the fluorescence intensity is higher in uncalendered paper than in calendered paper. This occurs because the light scatters more efficiently from uncalendered coatings.

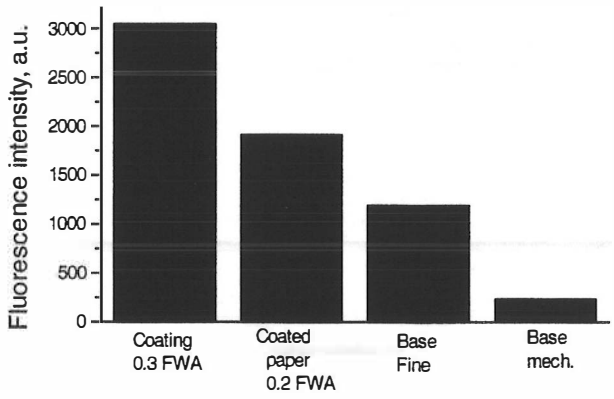

Figure 5.35. Fluorescence intensities of various samples.

The intensity of fluorescence depends on the concentration of fluorescent molecules. Absorption, scattering and reflection of the exciting and fluorescent light reduce the fluorescence intensity. Paper made of mechanical pulp contains lignin which fluoresces but on the other hand it also absorbs the fluorescent light and the net fluorescence emission is less than that of paper made of chemical pulp. Relative intensities of fluorescence of some samples are shown in Fig. 5.35.

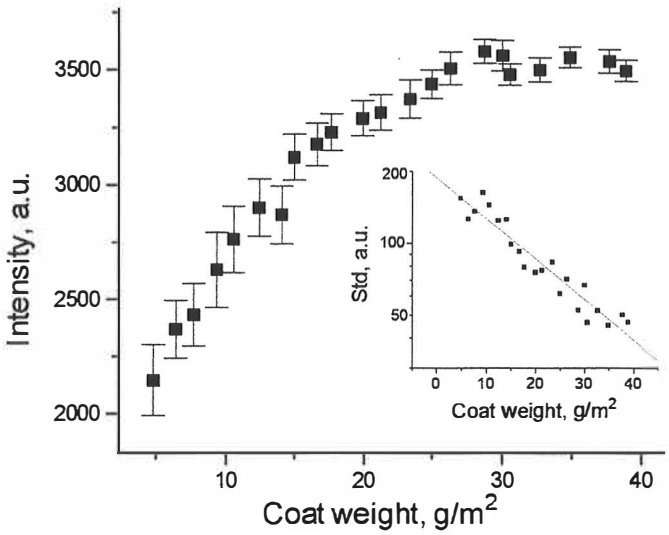

Figure 5.36. The fluorescence intensity and the standard deviation as a function of coat weight in coated paper (kaolin/ $CaCO_3$ coating on mechanical base paper)

The feasibility of LIF-method in the study of coated papers was tested by analyzing four sets of samples in which coat weight was varied from 2 to 40 g/cm^2. The samples were single, double, and triple coated depending on the coat weight. Base paper used for coating was LWC (mechanical) and in one case fine paper (chemical). In all samples the FWA was added in the coating. The fine base paper included FWA but LWC base papers did not. The fluorescence intensity increases as a function of coat weight in all cases while at the same time the standard deviation shows a decline (Fig. 5.36). The latter is due the logarithmic dependence of intensity on coat weight (Fig. 5.37). The variation of coat weight increases until the full coating coverage is obtained as shown in the histograms of Fig. 5.38.

Table 5.2. Content of samples.

	Base	Pigment
1	mcch	kaolin
2	chem.	kaolin
3	mech.	$CaCO_3$
4	mech	kaolin/$CaCO_3$ 50/50

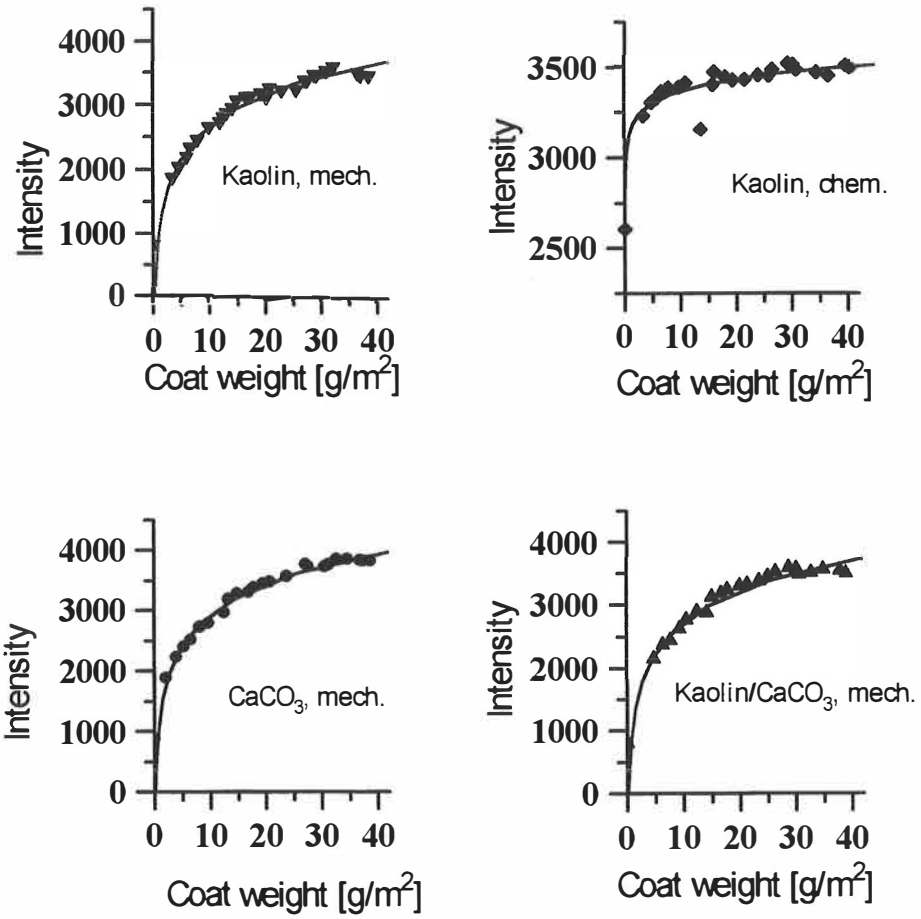

Figure 5.37. Fluorescence intensity as a function of coat weight in coated papers.

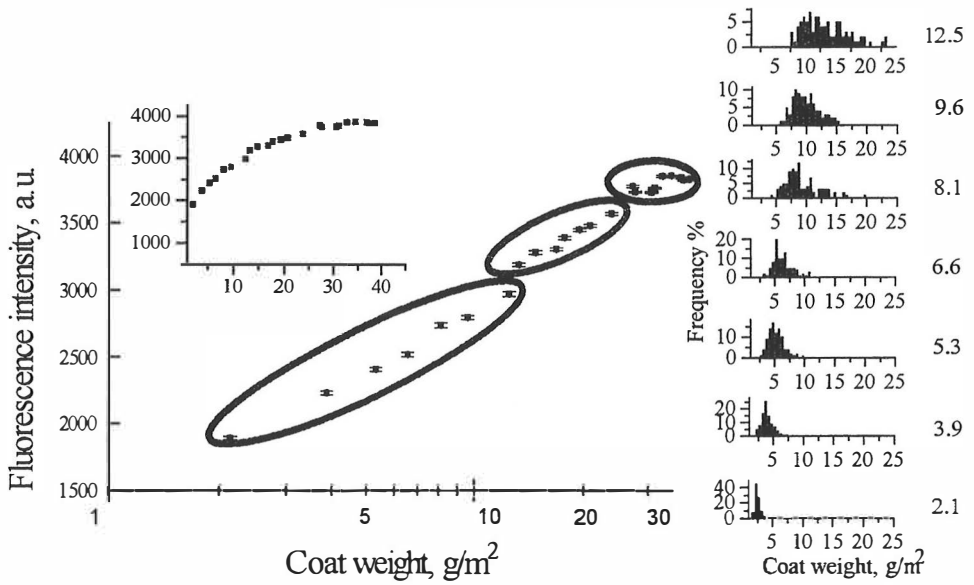

Figure 5.38. Fluorescence intensity as a function of coat weight (in logaritmic and linear scales) of single (red circle), double (green) and triple (blue) coatings. On the right the histogram presentations of coat weight distribution are shown for single coated papers.

For fine papers the coat weight ranges that are useful for LIF analysis vary in the range of 0-10g/m^2. Analysis of coat weight distributions on mechanical base paper was possible up to coat weights of 30 g/m^2. Pigment composition of the coating did not give any restriction for the analysis. The maximum coat weight for single coating was about 12 g/m^2. In Fig. 5.38 it is shown that the papers with single, double and triple coatings give slightly different response slopes. This may be due to differences in coating color or in the drying conditions.

5.4 LIF- VS. LIPS-ANALYSIS

The laser-induced plasma spectroscopy was initially used to confirm the interpretation of the results obtained by laser-induce fluorescence for coated papers, i.e. whether coat weight distributions in some grades could be analyzed by the LIF-method. This was considered to be of importance since LIF-method is non-destructive and thus suitable for on-line analysis. For more detailed analysis laser-induced plasma spectroscopy is preferable. It gives a good picture of the distribution of coating components in three dimensions.

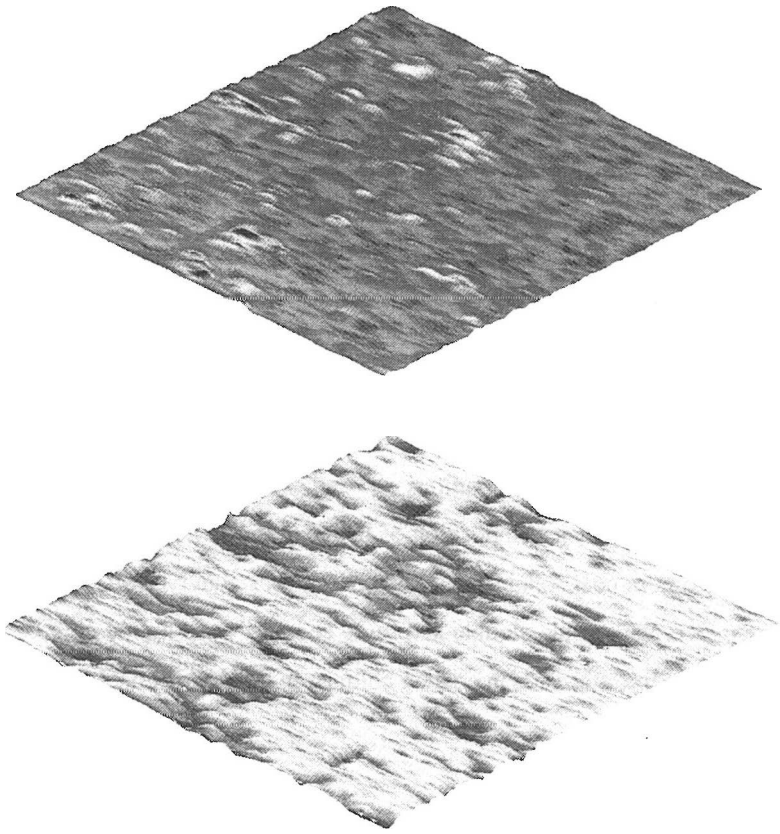

Figure 5.39. Coat weight distribution of coated paperboard by LIF(top) and LIPS (down).

Both methods were used to study the coat weight distribution of a coated paperboard sample where optical brightener was added in the base sheet. First the fluorescence intensities were recorded at a wavelength of 422 nm by using non-destructive low intensity excitation (1 % of that used for LIPS). Excitation energy was then increased and the same area was analyzed

by the LIPS-method. The atomic emission of silicon line at 251 nm was monitored. The fluorescence and the ablation images were created. In the studied paper board sample the fluorescence image proved to be an almost perfect mirror image of the LIPS image. The images shown in Fig. 5.39 support the interpretation that areas of high fluorescence intensity are less rich in pigment. The same areas in the LIPS image are low in pigment content. This suggests that laser induced fluorescence imaging is a feasible method for on-line measurement of coat weight distribution of paper grades that have intensive enough fluorescence from the base paper. The result also suggest that the excimer laser radiation can penetrate through the coating all the way to the base paper and that the fluorescence imaging gives a reliable picture of thickness variations of paper coatings.

The laser-induced fluorescence imaging is a feasible in-situ analysis method of coat weight distributions for some paper and paper board grades. It is quite easy to bring the laser light on the paper web via optical fiber and collect the fluorescent light to the detector via the same/or an additional fiber. It is also possible to use LIF for monitoring the amount of coating on the applicator roll before the coating event.

6 CONCLUSIONS

The material distributions in paper and paper coatings are important factors which determine the properties and quality of paper. In this thesis the main emphasis was on the development of a rapid and easy-to-use method for analysis of material distributions of coated paper. Two methods were developed. First the laser-induced fluorescence imaging method (LIF), which was used to study material distribution in x- and y-directions with spatial resolution of 0.1 mm in about 30 µm thick coating layer. LIF-method can be used for analysis of coat weight distribution in papers and paper boards where optical brighteners have been applied either in coating or in the base sheet. The on-line analysis of coat weight is also possible by using the LIF-method.

Secondly laser-induced plasma spectrometry was developed and it was used in the analysis of coat weight distributions. Both single and multilayer coatings were analyzed. The multilayer coatings which differ in their plasma emission spectra may be spatially separated by the method, if the compositions of pigments or the binder concentrations are different in the coating layers. The method allows for the estimation of coating coverage. The spatial resolution in the analysis is typically 0.1 mm in x- and y-directions and 2 µm in the z-direction. The measurement of coat weight distribution along a line 10 cm of length with resolution of 0.1 mm from 10 consecutive 2 µm layers takes about half an hour.

The main advantages of the method is that no sample preparation is needed. It measures the coat weight, pigment and binder distributions. Spatial resolution of measurement is of the order of printing dot size and sufficiently large areas may be analyzed in a reasonable time.

LIPS-method has already proved its feasibility in analyzing a wide variety of properties of coated and base papers. However, the potential of the method has not yet been fully realized. This requires more work in close cooperation with the papermakers.

7 REFERENCES

1. M. J. Whalen-Shaw Ed., *Binder Migration in Paper and Paperboard Coatings,* Tappi Press, Atlanta (1993).

2. B. L. Browning, *Analysis of Paper* 2nd edn., Marcel Dekker Inc., NewYork (1977).

3. J.-P. Bernié and W. J. M. Douglas, Tappi J. **79**(1),193 (1996).

4. G. Engström and J. Lafaye, Tappi J. **75**(8),117 (1992).

5. T. Arai, T. Yamasaki, K. Suzuki, T. Ogura, and Y. Sakai, Tappi J. **71**(59,47 (1988).

6. H.Fujiwara and J. E. Kline, Tappi J. **70**(12), 97 (1987).

7. C. Voillot, M. Gravier, A. Ramaz and J. M. Chaix, Tappi J. **73**(5), 109 (1990).

8. R. A. Peterson and C. L. Williams, Tappi J. **75**(10),122 (1992).

8. C. Guyot and B. Amram, 16th PTS coating symposium (1993).

9. T. Hattula and P.-J. Aschan Paperi ja Puu , **63,** 387 (1981).

10. I. Kartovaara, Paperi ja Puu **71**, 1033 (1989).

11. F. Brech and L. Cross, Appl. Spectrosc. **16**, 59 (1962).

12. R. H. Scott and A. Strasheim, in *Applied Atomic Spectroscopy*, E: L.Grove , ed. Plenum Press, New York, (1978) ,vol 1.

13. L. Moenke-Blankenburg, Prog. Anal. Atom. Spectrosc. **9**, 335 (1986).

14. E. H. Piepmeier, Laser Ablation for Atomic Spectroscopy , in *Analytical Applications of Lasers*, E. H. Piepmeir, Ed., John Wiley & Sons, New York (1986) chap.19 p. 627.

15. D. A. Cremers and L. J. Radziemski, *Laser Spectroscopy and its Application* L. J. Radziemski, R. W. Solarz and J. A. Paisner Eds., Marcel Dekker, New York, (1987).

16. L. J. Radziemski and D. A. Cremers Eds., *Laser-Induced Plasmas and Application*s Marcel Dekker, New York (1989).

17. J. C. Miller Ed., *Laser Ablation, Principles and Applications*, Springer-Verlag, Heidelberg (1994).

18. K. Y. Yamamoto, D. A. Cremers, M. J. Ferris, and L. E. Foster, Appl. Spectrosc. **50**, 222 (1996).

19. C. J. Lorenzen, C. Carlhoff, U.Hahn and M. Jogwich, J. Anal. At. Spectrom. **7**, 1029 (1992).

20. C.M. Davies, H.H. Telle, and A. W. Wlliams,Fresenius' J. Anal. Chem. **355**, 895 (1996).

21. W. Sdorra, J. Burst, and K. Niemax, Mikrochim. Acta **108**,1 (1992).

22. R. K. Singh and J. Narayan, Phys. Rew. B **41**, 8843 (1990).

23. B. Nemet, L. Kozma, Spectrochim. Acta **50 B**,1869 (1995).

24. R. S. Adrain and J. Watson, J. Phys. D **17**, 1915 (1984).

25. H. J. Häkkänen and J .E .I. Korppi-Tommola, Appl. Spectrosc. **47**, 2122 (1993).

26. H. J. Häkkänen and J .E .I. Korppi-Tommola, Appl. Spectrosc. **49**, 1721 (1995).

27. H. J. Häkkänen and J .E .I. Korppi-Tommola, Anal. Chem. (submitted 1998).

28. Y. Iida, Appl. Spectrosc. **43**, 229 (1989).